The Plant Cell, Vol. 19: 3194–3211, October 2007, www.plantcell.org © 2007 American Society of Plant Biologists

Manipulation of Phytoene Levels in Tomato Fruit: Effects on Isoprenoids, Plastids, and Intermediary Metabolism [W]

Paul D. Fraser,[a] Eugenia M.A. Enfissi,[a] John M. Halket,[b] Mark R. Truesdale,[a,1] Dongmei Yu,[a,2] Christopher Gerrish,[a] and Peter M. Bramley[a,3]

[a] School of Biological Sciences, Royal Holloway, University of London, Egham, Surrey, TW20 OEX, United Kingdom
[b] Specialist Bioanalytical Services Laboratory, Royal Holloway, University of London, Egham, Surrey, TW20 OEX, United Kingdom

In tomato (*Solanum lycopersicum*), phytoene synthase-1 (PSY-1) is the key biosynthetic enzyme responsible for the synthesis of fruit carotenoids. To further our understanding of carotenoid formation in tomato fruit, we characterized the effect of constitutive expression of an additional tomato *Psy*-1 gene product. A quantitative data set defining levels of carotenoid/isoprenoid gene expression, enzyme activities, and metabolites was generated from fruit that showed the greatest perturbation in carotenoid content. Transcriptional upregulation, resulting in increased enzyme activities and metabolites, occurred only in the case of *Psy*-1, *Psy*-2, and lycopene cyclase B. For reactions involving 1-deoxy-D-xylulose5-phosphate synthase, geranylgeranyl diphosphate synthase, phytoene desaturase, ζ-carotene desaturase, carotene isomerase, and lycopene β-cyclase, there were no correlations between gene expression, enzyme activities, and metabolites. Perturbations in carotenoid composition were associated with changes in plastid type and with chromoplast-like structures arising prematurely during fruit development. The levels of >120 known metabolites were determined. Comparison with the wild type illustrated that key metabolites (sucrose, glucose/fructose, and Glu) and sectors of intermediary metabolism (e.g., trichloroacetic acid cycle intermediates and fatty acids) in the *Psy*-1 transgenic mature green fruit resembled changes in metabolism associated with fruit ripening. General fruit developmental and ripening properties, such as ethylene production and fruit firmness, were unaffected. Therefore, it appears that the changes to pigmentation, plastid type, and metabolism associated with *Psy*-1 overexpression are not connected with the ripening process.

INTRODUCTION

During the ripening of tomato fruit (*Solanum lycopersicum*), coordinated genetic and biochemical events occur that result in changes to fruit texture, flavor, aroma, and color (reviewed in Alexander and Grierson 2002; Giovannoni, 2004). Tomato is a climacteric fruit; thus, ripening is distinguished by increased respiration and ethylene formation. Characterization of transgenic tomato plants in which ethylene production has been downregulated has shown that ethylene is required for normal fruit ripening (Picton et al., 1993). The dramatic color changes that occur during fruit ripening arise from the degradation of chlorophyll and accumulation of the acyclic carotenoid lycopene, which is responsible for the red coloration of ripe tomato fruit.

Carotenoids are isoprenoids and are all derived from isopentenyl diphosphate (IPP). Synthesis of carotenoids occurs in the plastid, using IPP formed via the methylerythritol-4-phosphate (MEP) pathway, not the extraplastidic mevalonate pathway (Rodriguez-Concepcion and Boronat, 2002; see Supplemental Figure 1 online). Geranylgeranyl diphosphate (GGPP) is the ubiquitous isoprenoid precursor in the formation of carotenoids. Phytoene synthase is the enzyme responsible for the conversion of GGPP to phytoene. This step has been subjected to upregulation by genetic manipulation (Fraser and Bramley, 2004). Two phytoene synthases exist in tomato, PSY-1 and PSY-2, the latter being predominantly responsible for carotenoid formation in chloroplast-containing tissues, while *Psy*-1 shows ripening-enhanced expression and is responsible for carotenoid formation in fruit ripening, although *Psy*-2 can still be detected in ripe tomato fruit (Fraser et al., 1999). Constitutive expression of *Psy*-1 in tomato results in pleiotropic effects, including cosuppression in ripening fruit and dwarfism due to the redirection of GGPP from gibberellins to carotenoids (Fray et al., 1995). Besides carotenoids and gibberellins, GGPP is also a precursor for chlorophyll and tocopherol formation (see Supplemental Figure 1 online). To overcome these pleiotropic effects and generate a high carotenoid– containing tomato fruit, a bacterial phytoene synthase (*crt*B) has been expressed in a fruit-specific manner, thus alleviating the detrimental pleiotropic effects previously encountered (Fraser et al., 2002).

Lycopene is the acyclic carotenoid formed from the sequential desaturation of phytoene. These reactions are catalyzed by the enzymes phytoene desaturase (PDS) and ζ-carotene desaturase (ZDS). The desaturase sequence occurs in the *cis* geometric isomer configuration, and the action of a carotene isomerase

[1] Current address: Genetix, Queensway, New Milton, BH25 5NN, UK.
[2] On leave from Lioaning Economic Forest Institute, No. 252 Yulin Street, Gangjingzi District, Dalian 116033, People's Republic of China.
[3] Address correspondence to p.bramley@rhul.ac.uk.
The author responsible for distribution of materials integral to the findings presented in this article in accordance with the policy described in the Instructions for Authors (www.plantcell.org) is: Peter M. Bramley (p.bramley@rhul.ac.uk).
[W] Online version contains Web-only data.
www.plantcell.org/cgi/doi/10.1105/tpc.106.049817

(CRTISO) converts either *cis*-neurosporene or poly-*cis* lycopene to all-*trans* lycopene prior to cyclization (Isaacson et al., 2004). In green tissue, the action of light and chlorophyll are believed to overcome the necessity for CRTISO activity (Isaacson et al., 2002; see Supplemental Figure 2 online). Cyclization of lycopene in tomato fruit yields β-carotene via the action of two β-cyclase enzymes. LCY-B is believed to predominate in the formation of vegetative carotenoids, while the *Cyc-B* gene shows ripening-specific expression and is thus associated with β-carotene production during ripening (Ronen et al., 2000). In vegetative tissues, α-carotene is formed via the action of a ε-ring cyclase and β-ring cyclase (Cunningham and Gantt, 2001). In ripe tomato fruit, xanthophyll formation occurring from the introduction of oxygen moieties into cyclic precursors is not an active part of metabolism. By contrast, in vegetative tissue, xanthophylls are the predominant carotenoids (see Supplemental Figure 2 online). For example, lutein is formed from α-carotene via the action of both β- and α-carotene hydroxylases (Tian et al., 2004; Fiore et al., 2006; Kim and DellaPenna 2006). Zeaxanthin is formed from β-carotene by the action of β-carotene hydroxylases. The conversion of zeaxanthin to neoxanthin (the precursor for abscisic acid) arises from the action of zeaxanthin epoxidase, yielding violaxanthin, from which neoxanthin is formed by neoxanthin synthase (Hirschberg, 2001; DellaPenna and Pogson, 2006; see Supplemental Figure 2 online).

In higher plants, carotenoids perform a variety of roles apart from ancillary photosynthetic pigments, free-radical scavengers (Demmig-Adams and Adams, 2002), and precursors of abscisic acid (Schwartz et al., 2003). In addition, it has recently been postulated that carotenoid-derived regulators of shoot branching exist (Booker et al., 2004), and in tomato, carotenoids are important precursors of aroma/flavor volatiles (Simkin et al., 2004). Besides roles in plant processes, carotenoids are an essential component of human nutrition. For example, deficiency of β-carotene (provitamin A) will result in blindness and eventually death (Mayne, 1996), while other carotenoids, such as lycopene and zeaxanthin/lutein, have been implicated in reducing the onset of certain cancers and age-related macular degeneration, respectively (Landrum and Bone, 2001; Giovannucci, 2002). Ripe tomato fruit and its products are the principal source of lycopene in the Western diet as well as an important source of β-carotene, flavonoids, phenolics, and tocopherols. Thus, there is an important biotechnological interest in increasing/altering carotenoids in tomato fruit and other crop plants to improve consumer health and color and organoleptic quality traits. In this article, we used transgenic tomato plants where the coordinated process of pigment production and ripening in fruit has been altered by genetic modification to demonstrate the implications at the metabolite and cellular level.

RESULTS

Generation of Transgenic Tomato Plants Expressing *Psy*-1 in a Constitutive Manner

Thirty-seven PCR positive primary transformants expressing endogenous tomato *Psy*-1 under the cauliflower mosaic virus (CaMV) constitutive 35S promoter control were generated. Within this population, some dwarf phenotypes were observed along with paler flower color and bleached green fruit. Ripe fruits were produced by 30 plants, 18 of which were red in color. Of the remaining 12 plants, fruit color ranged from yellow to yellow with blotchy red sectors. Compared with the wild type, the carotenoid content of the yellow fruit was ~100-fold less and only five out of the 18 red colored ripe fruit exhibited significant increases (1.2- to 1.5-fold) in carotenoid content (see Supplemental Table 1 online). The predominant carotenoids responsible for these increases were phytoene (1.5- to 3.0-fold), lycopene (up to 1.5-fold), and β-carotene (1.5- to 3.0-fold). The subpopulation of transgenic plants with elevated carotenoid contents has been the focus of the study (i.e., lines PS1-C38, PS1-C24, PS1-C17, PS1-C14, and PS1-C26).

Homozygous progeny were selected from primary transformants showing elevated carotenoid content by DNA gel blotting and germination on kanamycin. Interestingly, some lines with exclusively red colored ripe fruit in the T0 yielded some plants with yellow colored fruit in the T1 generation, while other plants retained a red ripe fruit phenotype. The primary transformants PS1-C14 and -C26 contained a single but different transgene insert and exhibited the greatest increases in carotenoid content. Progeny from these transformants exhibited approximate Mendelian inheritance (i.e., azygous 22 to 33%, hemizygous 48 to 55%, and homozygous 20 to 22%). Nine homozygous lines were generated from two primary lines of interest. All these homozygous lines showed premature pigmentation (yellow/pink) at the mature green stage of ripening. This phenotype was also displayed to a varying degree in all 20 hemizygous plants but not evident in the azygous or wild-type plants (see Supplemental Table 1 online). Total carotenoids in mature green fruit from the homozygous lines had increased levels (up to 1.7-fold), principally due to elevated levels of phytoene, phytofluene, lycopene, and β-carotene (see Supplemental Table 1 online). Ripe fruit from homozygous lines and hemizygous lines contained increased total carotenoid levels, although in some cases the increases were not statistically significant compared with wild-type or azygous control fruit. To create a stable variety displaying premature pigmentation that could be used to elucidate regulatory mechanisms involved in carotenoid formation during tomato fruit development and ripening and be used as a background for stacking carotenoid genes, the homozygous line PS1-C26R2 was grown and analyzed over a minimum of six generations, with three to six plants per crop. In all cases, the phenotype was inherited (see Supplemental Table 1 online), and this line has been used in this study to characterize and elucidate the effects of an additional *Psy*-1 on isoprenoids, plastids, and intermediary metabolism.

Extreme phenotypic effects on plant development have previously been reported following constitutive *Psy*-1 expression in tomato, such as loss of vigor, dwarfism, spindly vegetative tissue, and smaller fruit (Fray et al., 1995). However, besides premature pigmentation in the T1 generation, no extreme phenotypic differences were observable for the lines showing elevated carotenoids in the ripe fruit (PS1-C38, PS1-C24, PS1-C17, PS1-C14, and PS1-C26). A comparison of general phenotypic parameters of the wild-type and transgenic *Psy*-1 varieties is provided in Supplemental Table 2 online. Plant height, fruit yield, and seed index were all unaffected.

Alterations in Carotenoid Content during Fruit Development and Ripening Resulting from Transgenic *Psy*-1 Expression

To ascertain the changes in carotenoid content arising from constitutive expression of *Psy*-1, quantitative profiling of carotenoids was performed on developing and ripening fruit. The wild-type (Ailsa Craig) background was used as the comparator for the transgenic *Psy*-1 variety and five stages of fruit development and ripening sampled (i.e., immature green, mature green, breaker, turning, and ripe). During the development and ripening of tomato fruit, the characteristic change from chloroplast pigments (e.g., chlorophylls and xanthophylls) found at the immature and mature green stage to pigments associated with the chromoplasts of ripe fruit (phytoene and lycopene) occurred in the wild type. In the *Psy*-1 transgenic variety, this qualitative profile was altered at the immature and particularly mature green stages (Figures 1A to 1H). The profiles gave 54 components (see Supplemental Table 3 online), most of which possessed characteristic carotenoid signature spectra. In the mature green samples, a number of carotenoids unique to the *Psy*-1 transgenic variety were observed, including an isomer of neoxanthin, phytoene (four isomers), phytofluene (seven isomers), ζ-carotene (three isomers), α-carotene, δ-carotene (two isomers), γ-carotene, and lycopene (five isomers), as indicated in bold in Supplemental Table 3 online. By contrast, a comparison between the carotenoids in ripe wild type and the *Psy*-1 fruit showed few qualitative differences. Collectively, 72 components were detected in ripe fruit, of which 58 were carotenoids, and 47 of known identity (see Supplemental Table 4 online).

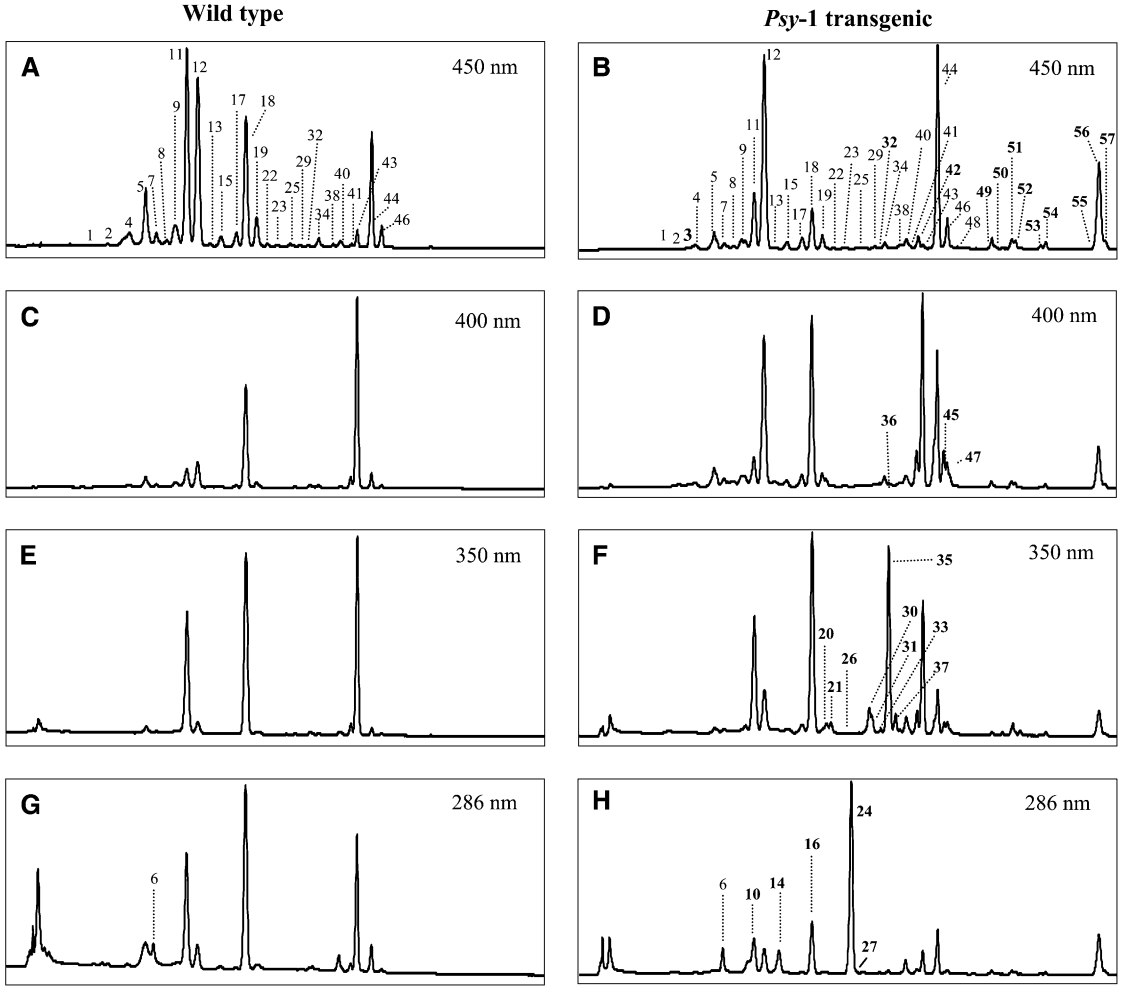

Figure 1. Profiles of Carotenoids and Other Isoprenoids Present in Both *Psy*-1 and Wild-Type Fruit at the Mature Green Stage.

(A) and **(B)** Chromatograms for the wild type and *Psy*-1 variety [PS1-C26R2 (T_7)], respectively, recorded at 450 nm.
(C) and **(D)** Wild type and *Psy*-1 chromatograms recorded at 400 nm, respectively.
(E) and **(F)** Chromatograms recorded at 350 nm for the wild type and *Psy*-1 variety, respectively.
(G) and **(H)** Chromatograms from the wild type and *Psy*-1 variety recorded at 286 nm.
Chromatogram components are numbered, and those in bold represent components unique to *Psy*-1. For peak identity, UV/Vis spectral characteristics, and chromatographic properties, see Supplemental Table 1 online. The mature green stage used for this analysis represents 36 d after anthesis.

The levels of the predominant carotenoids and chlorophylls during fruit development and ripening of the *Psy*-1 and wild type are shown in Table 1. The carotenoid and chlorophyll contents of the *Psy*-1 immature fruit increased by 2-fold and 1.8-fold, respectively, but the carotenoid-to-chlorophyll ratio was not altered significantly nor the composition of chlorophyll A and B, β-carotene, lutein, neoxanthin, and violaxanthin. Phytoene, phytofluene, ζ-carotene, and lycopene were only found in the *Psy*-1 variety at this immature stage of fruit development. At the mature green stage, dramatic alterations in the carotenoid composition occurred in the *Psy*-1 variety. The total content of carotenoids was 6.7-fold greater in the *Psy*-1 fruit. In contrast with the immature fruit, chlorophyll levels in the *Psy*-1 variety were reduced 3.7-fold in *Psy*-1 fruit. Collectively, this altered the carotenoid-to-chlorophyll ratio some 25-fold. The increases in the carotenoid content of the *Psy*-1 mature green fruit are principally due to elevations in β-carotene and lutein of 26.2- and 2.4-fold, respectively. With the exception of lycopene, present at a low level (0.24 ± 0.01 μg per g dry weight), acyclic carotenes remained absent in the wild-type mature green fruit, while *Psy*-1 mature fruits contain significant levels of acyclic carotenoids.

With the onset of fruit ripening at the breaker stage, increased carotenoid content (7.0-fold) was found in the *Psy*-1 fruit compared with the wild type. Chlorophyll levels were reduced in the wild type and the *Psy*-1 fruit by 2.5- and 15.3-fold, respectively, resulting in a dramatic increase in the carotenoid-to-chlorophyll ratio to 507.2 compared with 3.2 in the wild type. Although phytoene and lycopene were detectable at this ripening stage, their levels were low compared with *Psy*-1 fruit. As ripening proceeds to the turning stage, phytoene, phytofluene, ζ-carotene, lycopene, and β-carotene levels in the *Psy*-1 fruit were all greater compared with wild-type levels. Lutein, neoxanthin, and violaxanthin contents were virtually unaltered among the wild-type and *Psy*-1 fruit. Collectively, the *Psy*-1 fruit at this ripening stage contained 3.5-fold more carotenoids. The principal carotenoid in the wild-type fruit at this ripening stage was lycopene, while in the *Psy*-1 fruit, β-carotene persisted as the predominant carotenoid. Lycopene was the predominant carotenoid in both wild-type and *Psy*-1 ripe fruit, with no difference in its level between varieties. The total carotenoid content and composition of the *Psy*-1 and wild-type ripe fruit was not altered significantly.

During the development and ripening of wild-type fruit, the burst in carotenoid formation occurred from the breaker to turning fruit stages, but in the *Psy*-1 variety, the most intense period of phytoene, phytofluene, and β-carotene synthesis occurred from the immature to mature green stages. However, lycopene formation did not follow this trend, showing an accumulation from the breaker to turning stage. Chlorophyll A showed the most dramatic fall in content within the fruit. Despite the initial perturbations in carotenoid content during development, by the onset of ripening, homeostasis of the carotenoid content has been achieved. The quantitative and qualitative carotenoid content of the *Psy*-1 variety was virtually identical to the wild type with the exception of the presence of phytoene.

Effect of Constitutive *Psy*-1 Expression on Isoprenoid Gene Expression and Enzyme Activities

The profiling of carotenoids during fruit development and ripening indicated that the *Psy*-1 mature green fruit showed the most pronounced effects of metabolite perturbation. Therefore, this stage was our primary focus to ascertain alterations at the gene expression and enzyme level that lead to unscheduled pigmentation in the fruit.

In wild-type fruit, the relative extent of gene expression indicated that *Dxs*, *Gggps*-1, and *Zds* were the most abundant transcripts (1.0 to 2.5 relative amount), and *Psy*-1, *Ggpps*-2, *Psy*-2, *Lcy*-B, *CrtISO*, and *Pds* were all expressed at a similar level (0.08 to 0.3 relative amount), with the *Cyc*-B gene showing a lower transcript abundance (0.005 relative amount). Comparisons between the expression of these genes in the *Psy*-1 variety with the wild type indicated that the expression of *Ggpps*-1 and -2, *Pds*, and *Lcy*-B were not significantly altered (Figure 2A). The level of this transcript was elevated 15-fold. Other transcripts elevated in this line included *Psy*-2 (4-fold) and the *Cyc*-B gene (4-fold). *Dxs*, *Zds*, and *CrtISO* all showed significantly reduced transcript levels (0.6-fold; Figure 2A).

Increases in phytoene synthase and lycopene cyclase activities in vitro were found (Figure 2B). In contrast with its transcript

Table 1. Carotenoid and Chlorophyll Content of *Psy*-1 and Wild-Type Tomato Fruit during Development and Ripening

	Carotenoid and Chlorophyll Contents (μg/g DW)									
	Immature		Mature Green		Breaker		Turning		Ripe	
Carotenoid/Chlorophyll	Wild Type	*Psy*-1	Wild Type	*Psy*-1	Wild Type	*Psy*-1	Wild Type	*Psy*-1	Wild Type	*Psy*-1
Phytoene	0.0 ± 0.0	6.5 ± 0.6 (2.2)	0.0 ± 0.0	133.1 ± 13.9 (14)	6.0 ± 0.2 (3.6)	161.0 ± 10.2 (13.5)	102.3 ± 0.8 (6.5)	164.5 ± 10.5 (11.0)	102.3 ± 3.7 (5.6)	240.2 ± 9.9 (11)
Phytofluene	0.0 ± 0.0	2.2 ± 0.2 (0.8)	0.0 ± 0.0	51.5 ± 5.5 (5.5)	0.0 ± 0.0	74.8 ± 4.7 (6.0)	2.6 ± 0.05 (0.6)	67.7 ± 4.3 (4.6)	51.3 ± 1.9 (2.8)	91.6 ± 5.8 (4.0)
ζ-Carotene	0.0 ± 0.0	0.0 ± 0.0	0.0 ± 0.0	18.8 ± 2.0 (2.0)	0.0 ± 0.0	79.2 ± 5.0 (6.6)	6.0 ± 0.2 (1.4)	23.0 ± 1.5 (1.5)	16.1 ± 0.6 (0.9)	22.8 ± 11.5 (1.0)
Lycopene	0.0 ± 0.0	34.9 ± 3.0 (11.9)	0.24 ± 0.01 (0.2)	25.3 ± 2.7 (2.7)	2.7 ± 0.1 (1.6)	96.1 ± 6.1 (8.0)	165.8 ± 4.0 (39.0)	433.9 ± 27.4 (29.2)	949.45 ± 33.95 (52)	964.9 ± 55.9 (42)
β-Carotene	40.5 ± 2.6 (24)	134.6 ± 12.0 (45.9)	17.3 ± 0.6 (12.3)	452.7 ± 47.7 (48)	61.2 ± 4.3 (36.8)	637.5 ± 40.5 (53)	115.5 ± 7.3 (27.0)	666.0 ± 42.1 (44.8)	586.2 ± 21.0 (32.3)	819.3 ± 51.3 (36)
Lutein	85.7 ± 5.5 (51)	100.4 ± 8.7 (34)	94.8 ± 6.6 (68)	224.3 ± 14.2 (24)	78.2 ± 2.9 (47.0)	134.5 ± 14.5 (11)	99.7 ± 2.4 (23.0)	115.5 ± 7.3 (7.8)	99.6 ± 3.6 (5.5)	123.3 ± 7.7 (5.4)
Neoxanthin	14.1 ± 0.9 (8.3)	7.1 ± 0.6 (2.4)	15.4 ± 1.1 (11)	18.8 ± 1.2 (2.0)	9.4 ± 0.4 (5.6)	1.7 ± 0.2 (0.1)	6.6 ± 0.15 (1.5)	6.2 ± 0.4 (0.4)	2.4 ± 0.07 (0.13)	3.6 ± 0.2 (0.16)
Violaxanthin	28.1 ± 1.8 (16.7)	7.4 ± 0.6 (2.5)	12.7 ± 0.9 (9.1)	16.8 ± 1.1 1.8	8.8 ± 0.4 (5.3)	6.7 ± 0.3 (0.6)	6.3 ± 0.1 (1.5)	7.2 ± 0.0 (0.5)	4.7 ± 0.15 (0.3)	5.95 ± 0.4 (0.3)
Total carotenoid	168.4 ± 10.8	293.0 ± 24.7	140.4 ± 9.2	941.3 ± 88.3	166.3 ± 8.3	119.2 ± 81.5	430.6 ± 15	1484.0 ± 94.0	1812.0 ± 65	2276.7 ± 142.7
Chlorophyll A	26.5 ± 1.5 (41)	65.1 ± 5.5 (47)	40.4 ± 2.8 (30.6)	0.57 ± 0.04 (1.6)	0.6 ± 0.0 (1.2)	0.35 ± 0.04 (14.9)	1.7 ± 0.4 (4.0)	0.15 ± 0.01 (11)	0.2 ± 0.0 (7.1)	0.16 ± 0.01 (10)
Chlorophyll B	38.5 ± 2.4 (59)	74.4 ± 6.3 (53)	92.0 ± 6.4 (69.7)	35.2 ± 2.2 (98.6)	50.9 ± 1.8 (98.8)	2.0 ± 0.2 (85.0)	40.3 ± 0.95 (96)	1.2 ± 0.1 (86)	2.6 ± 0.1 (93)	1.4 ± 0.09 (88)
Total chlorophyll	64.9 ± 3.9	139.5 ± 11.8	132.0 ± 9.2	35.7 ± 2.24	51.5 ± 1.8	2.35 ± 0.24	42.0 ± 1.4	1.4 ± 0.1	2.8 ± 0.1	1.6 ± 0.1
Carotenoid:chlorophyll	2.6 ± 0.2	2.1 ± 0.2	1.06 ± 0.1	26.4 ± 1.6	3.2 ± 0.14	507.2 ± 43	10.2 ± 3.4	1060.0 ± 66.8	NA	NA

The *Psy*-1 variety PS-1C26R2 (T_7) was used. Immature is 11 ± 2 d after anthesis; mature green, 37 ± 1 d after anthesis; breaker, 44 ± 1 d after anthesis; turning, 3 d after breaker; ripe, 10 d after breaker. Three representative fruit from three plants were used for each developmental/ripening stage. The fruit were pooled and at least three determinations made per sample. The data are presented ± SE. DW, dry weight; NA, not applicable.

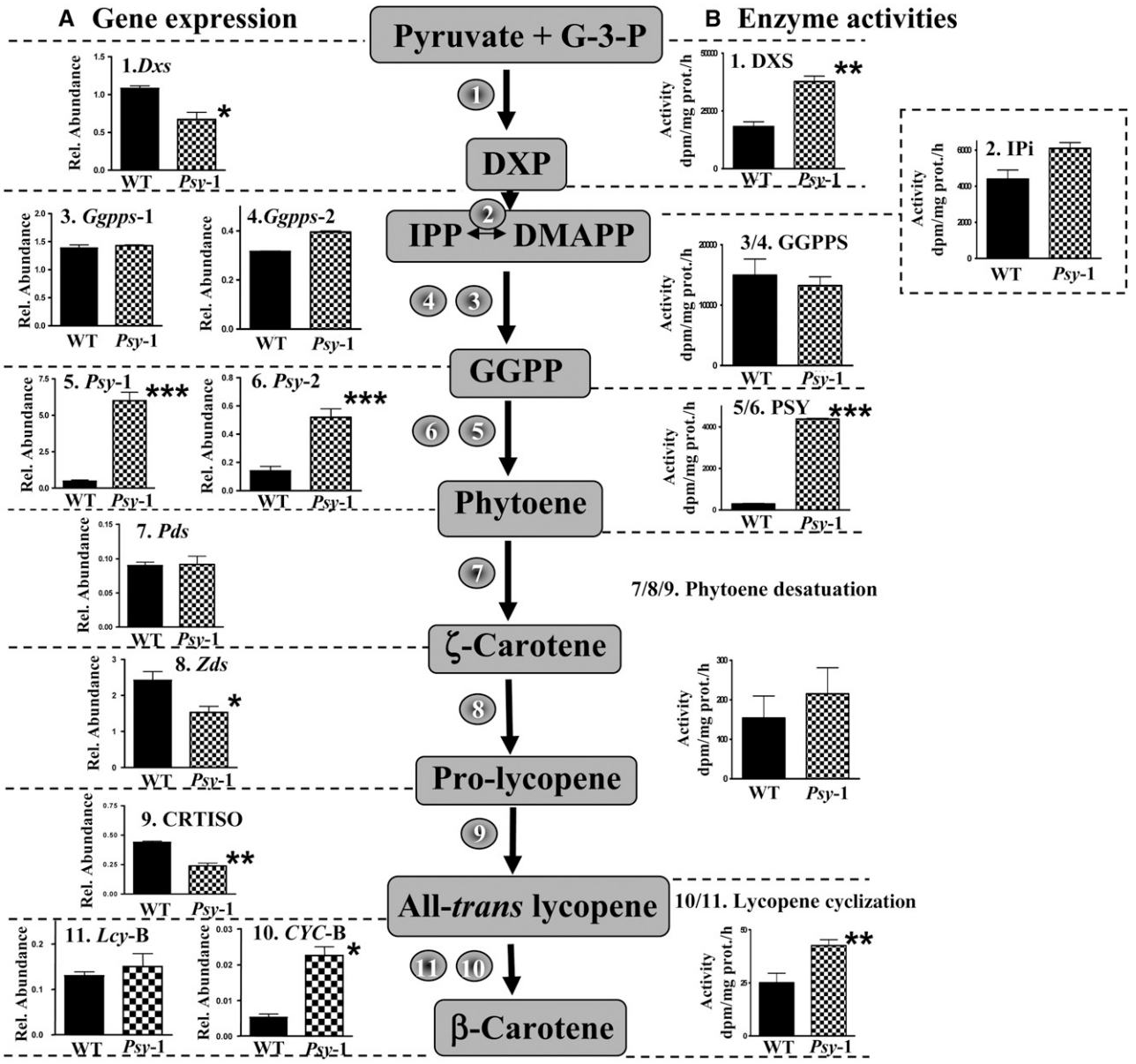

Figure 2. Changes in Isoprenoid/Carotenoid Gene Expression Levels and Enzyme Activities Resulting from the Expression of an Additional *Psy-1*.

The *Psy*-1 variety PS-1C26R2 (T_7) was used for the determination of gene expression and enzyme activity. One fruit (at the mature green stage, 36 to 37 d after anthesis) from three representative *Psy*-1 and wild-type plants was pooled and pulverized into a homogeneous powder as described in Methods. Total RNA was then extracted from an aliquot of this material. Quantitative real-time RT-PCR was performed with gene-specific primers for (1) *Dxs*, (3) *Ggpps*-1, (4) *Ggpps*-2, (5) *Psy*-1, (6) *Psy*-2, (7) *Pds*, (8) *Zds*, (9) *CrtISO*, (10) the *Cyc-B* gene, and (11) *Lcy*-B. Enzymes are numbered similarly, with the addition of (2) IPP isomerase. Expression data were normalized to the expression of actin. The data represent SE ± ($n = 3$ to 8). Student's *t* tests illustrate statistical significance (* $P < 0.05$, ** $P < 0.01$, and *** $P < 0.001$). The black bars indicate wild-type determinations, and the checkered bars are for the *Psy*-1 transgenic variety. Enzyme activities were performed on extracts determined from the same tissue used for RNA analysis. Specific assays for DXS, GGPPS, PSY, PDS, and lycopene cyclase were performed as described in Methods. The protein levels used were as follows: 440 μg for the *Psy*-1 and wild-type extracts used in the assays of phytoene desaturation and lycopene cyclization; 200 and 100 μg for the wild type and *Psy*-1 extracts, respectively, used to assay DXS, IPI, GGPPS, and PSY. Typically, substrate levels were ~50,000 dpm phytoene and 20,000 dpm lycopene formed from 1 μCi ^{14}C-IPP. In all cases, activity was expressed as dpm incorporated/mg protein/h. Determinations were performed at least in triplicate. Data are shown as SE ($n =$ at least 3).

level, 1-deoxyxylulose 5-phosphate synthase (DXS) activity was significantly elevated. Both GGPP synthase and phytoene desaturation activities in vitro were not altered. However, the composition of desaturase products formed from phytoene by the PSY-1 fruit membranes was different than the wild type. For example, ζ-carotene, lycopene, and β-carotene represented 10, 53, and 34% of the total in vitro desaturase products formed by wild-type extracts, while *Psy*-1 fruit had a profile of 19, 40, and 40% for ζ-carotene, lycopene, and β-carotene, respectively. Thus, desaturation in vitro indicated that a greater proportion of ζ-carotene and β-carotene, but not lycopene, was formed in the *Psy*-1 variety compared with the wild type.

Although *Psy*-1 ripe fruit carotenoids were not significantly increased, the expression of *Psy*-1 in this tissue was elevated some 2-fold and was accompanied by a modest but significant increase (2.5-fold) in phytoene synthase activity compared with the wild type.

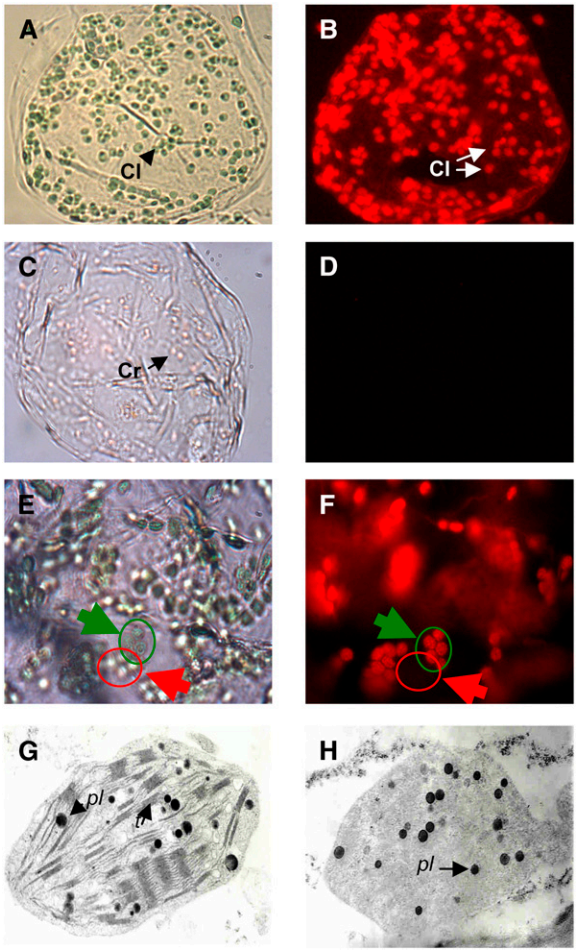

Figure 3. Visualization of Plastids Present in Wild Type and *Psy*-1 Variety.

The *Psy*-1 variety PS-1C26R2 (T_8) was used for this analysis. pl, plastoglobules; t, thylakoid grana; Cl, chloroplasts; Cr, chromoplasts.
(A) and **(B)** A typical wild-type cell from mature green fruit (36 d after anthesis) visualized under bright-field **(A)** and fluorescence emission **(B)** magnification ×10.
(C) and **(D)** A typical cell from *Psy*-1 mature green fruit (bottom section of fruit) visualized under bright-field and fluorescence emission, respectively, ×10.
(E) and **(F)** The higher magnification (×40) of the *Psy*-1–derived cell from the top section of the mature green fruit under bright-field and fluorescence emission, respectively. Green arrow shows plastids autofluorescing due to the presence of chlorophyll, and red arrow indicates collection of plastids in which chlorophyll is absent.
(G) and **(H)** Transmission electron micrographs of the wild type and *Psy*-1 variety, respectively.

The Effect of *Psy*-1 Expression on Plastid Type

Light and fluorescence microscopy studies were performed on fruit pericarp through development and ripening for wild-type and *Psy*-1 lines. As expected from visual observations, the most striking difference arose at the mature green stage. Figures 3A and 3B illustrate a typical cell from mature green fruit, populated with distinct chloroplast-like structures that appear green under bright-field and autofluorescence when viewed under the fluorescence microscope. Figures 3C and 3D represent light and fluorescence microscopy performed on pericarp tissue from the bottom of *Psy*-1 mature green fruit where chlorophyll disappearance is most pronounced. It can be seen clearly that the plastid-like structures are now pink in color (Figure 3C) and have no autofluorescence (Figure 3D). Because of the heterogeneity of chlorophyll content throughout the *Psy*-1 fruit, sections at the very top of the fruit, which contained higher chlorophyll contents, were also visualized. In this part of the fruit, populations of both types of plastid coexist. For example, in Figure 3E, the green arrow shows pink structures that do not autofluorescence (Figure 3F). Thus, both chloroplasts and chromoplasts coexist in the same cell. Sections prepared from ripe tissue appear similar to Figures 3C and 3D, and no observable differences were found between the two varieties. Cellular sections derived from immature fruit exhibited a greater similarity between wild-type and *Psy*-1 fruit, although distinct nongreen plastid-like structures were present, but not to the extent found in mature green fruit.

Figure 3G illustrates the presence of defined stacked thylakoid membranes containing the photosynthetic grana as well as dense-staining plastoglobuli. Compared with the typical chloroplast structures found in wild-type mature green fruit, plastids derived from *Psy*-1 mature green fruit showed the absence of distinct thylakoid membranes. Plastoglobuli remained in the plastid (Figure 3H). The population of each plastid species varied depending on where the fruit was sectioned (i.e., top or bottom), but it was clear that cells contained a heterologous population of plastids. The plastid ultrastructure in ripe fruit showed no observable difference between the modified plastids found in *Psy*-1 mature green fruit and ripe fruit except the presence of long crystalline structures (presumably lycopene) present in the ripe fruit (data not shown).

Metabolite Analysis of *Psy*-1 Fruit Compared with the Wild Type

As anticipated, characteristic changes in metabolites occur during fruit ripening (Table 2). Of the compounds analyzed,

Table 2. Relative Metabolite Levels in Wild Type and *Psy*-1–Overexpressing Fruit at the Mature Green and Ripe Stages of Fruit Development and Ripening

Metabolite	Wild-Type MG:*Psy*-1 MG	Wild-Type MG:Wild-Type Ripe	Wild-Type Ripe:*Psy*-1 Ripe	*Psy*-1 MG:*Psy*-1 Ripe
Organic acids				
Aconitic acid	**0.71 ± 0.05***	0.98 ± 0.30	0.69 ± 0.07	1.10 ± 0.10
Ascorbic acid	1.32 ± 0.30	**30.70 ± 4.80*****	1.40 ± 0.30	**32.40 ± 2.40*****
Citramalic acid	0.90 ± 0.03	**3.40 ± 0.30****	**3.20 ± 0.40*****	**11.80 ± 1.50****
Citric acid	**0.62 ± 0.1****	0.92 ± 0.02	**1.40 ± 0.03*****	**2.03 ± 0.24*****
Dehydroascorbic acid	**0.00 ND*****	**2.00 ± 0.22***	**2.20 ± 0.10*****	**~10.00#*****
Fumaric acid	**0.60 ± 0.08***	**0.20 ± 0.04*****	1.10 ± 0.11	**0.38 ± 0.02****
Galactonic acid	0.56 ± 0.03	1.00 ± 0.05	**0.80 ± 0.04***	**1.50 ± 0.07*****
Galacturonic acid	**0.00 ND*****	**1.80 ± 0.45***	**0.64 ± 0.04***	**~10.00#*****
Glucaric acid	**0.28 ± 0.05****	**0.09 ± 0.04****	0.98 ± 0.14	**0.30 ± 0.04*****
Glycerate	1.00 ± 0.20	**0.30 ± 0.00*****	1.20 ± 0.10	**0.20 ± 0.02*****
Glycolate	0.82 ± 0.07	**0.40 ± 0.07****	0.92 ± 0.10	**0.50 ± 0.04*****
Gluconic acid	0.97 ± 0.05	**1.90 ± 0.10****	**0.76 ± 0.07***	**1.50 ± 0.13****
Lactic acid	0.83 ± 0.10	**2.20 ± 0.17****	**1.40 ± 0.08****	**3.60 ± 0.40*****
Malic acid	0.80 ± 0.04	**0.32 ± 0.01*****	1.04 ± 0.03	**0.41 ± 0.01*****
Oxalic acid	**0.08 ± 0.01*****	**0.03 ± 0.00*****	1.60 ± 0.40	1.40 ± 0.20
2-Oxoglutaric acid	**0.00 ND*****	**0.05 ± 0.02***	2.60 ± 1.00	**~10.00#*****
Quinic acid	**0.20 ± 0.01****	**0.40 ± 0.01***	0.83 ± 0.08	**2.10 ± 0.21*****
Succinic acid	**0.60 ± 0.03***	**0.24 ± 0.01****	0.94 ± 0.06	**0.40 ± 0.02*****
Tartaric acid	0.82 ± 0.04	**3.00 ± 0.15****	1.10 ± 0.10	**3.90 ± 0.40*****
Threonic acid	1.10 ± 0.20	**0.50 ± 0.10***	0.70 ± 0.10	**0.60 ± 0.10***
Amino acids				
Ala	**2.00 ± 0.40***	**2.02 ± 0.40***	**1.50 ± 0.20***	**1.40 ± 0.08***
β-Ala	0.92 ± 0.10	**0.10 ± 0.02*****	**4.70 ± 1.80*****	**0.30 ± 0.03*****
4-Aminobutryic acid	0.90 ± 0.03	**0.10 ± 0.03*****	**3.50 ± 1.40*****	**0.30 ± 0.02*****
Asn	**7.50 ± 1.70***	**10.0 ± 1.20*****	**2.60 ± 0.43***	**25.60 ± 5.00****
Asp	1.50 ± 0.30	**2.80 ± 0.03****	**1.50 ± 0.10****	**2.60 ± 0.20*****
Cys	**0.00 ND*****	0.40 ± 0.20	**1.80 ± 0.30***	**~10.00#*****
Glu	**1.60 ± 0.20***	**4.60 ± 0.10*****	0.94 ± 0.01	**2.60 ± 0.27*****
Gln	1.30 ± 0.30	**0.46 ± 0.16***	**3.00 ± 0.30***	1.03 ± 0.40
Gly	1.00 ± 0.10	**0.14 ± 0.02*****	**4.10 ± 0.22*****	**0.55 ± 0.03****
5-Hydroytryptamine	1.40 ± 0.40	1.33 ± 0.10	1.40 ± 0.11	1.30 ± 0.14
Leu	**0.42 ± 0.01*****	**0.20 ± 0.00*****	**0.40 ± 0.02*****	1.00 ± 0.04
Lys	**2.20 ± 0.50***	**8.10 ± 0.30*****	1.10 ± 0.02	**4.00 ± 0.35*****
5-Oxo-proline	1.20 ± 0.20	**1.54 ± 0.08***	1.00 ± 0.10	1.30 ± 0.30
Ser	**0.70 ± 0.10***	**0.40 ± 0.08****	**3.10 ± 0.32*****	**2.00 ± 0.20****
Thr	0.85 ± 0.11	0.80 ± 0.10	**1.60 ± 0.08****	**1.30 ± 0.03***
Val	1.00 ± 0.15	**0.11 ± 0.02****	**3.50 ± 0.02*****	**0.40 ± 0.06****
Fatty acids				
Linoleic acid	**0.57 ± 0.03***	**0.11 ± 0.02*****	**1.80 ± 0.15****	**0.40 ± 0.05*****
Oleic acid	**0.38 ± 0.15***	**0.09 ± 0.02***	**1.90 ± 0.20***	**0.43 ± 0.05*****
Palmitic acid	**0.42 ± 0.01***	**0.15 ± 0.01****	**2.00 ± 0.07*****	**0.71 ± 0.02*****
Stearic acid	**0.23 ± 0.07***	**0.17 ± 0.02****	1.25 ± 0.07	0.90 ± 0.05
Sugars				
Arabinose	**9.30 ± 1.90*****	**9.30 ± 0.50*****	**2.90 ± 0.30****	**2.90 ± 0.10****
Deoxyxylulose-5-phosphate[a]	1.20 ± 0.04	–	–	–
Fructose	0.60 ± 0.14	**2.00 ± 0.20***	0.70 ± 0.08	**2.50 ± 0.30*****
Gentiobiose	**0.40 ± 0.07****	**2.80 ± 0.30****	**2.10 ± 0.30****	**15.2 ± 1.6*****
Glucose	1.20 ± 0.04	**1.83 ± 0.08****	**0.86 ± 0.04***	**1.30 ± 0.04*****
Maltose	**0.27 ± 0.007*****	0.82 ± 0.02	1.30 ± 0.17	**4.00 ± 0.40****
Melezitose	**0.15 ± 0.03****	**4.00 ± 0.05*****	0.70 ± 0.20	**18.7 ± 4.8***
Rhamnose	**580.50 ± 35.0*****	**1.40 ± 0.20***	1.20 ± 0.18	**0.01 ± 0.00*****
Ribose	**0.43 ± 0.04***	**1.50 ± 0.20***	1.00 ± 0.06	**3.70 ± 0.15*****
Sucrose	**0.50 ± 0.02*****	**0.65 ± 0.01****	**0.45 ± 0.05*****	**0.54 ± 0.03*****
Xylose	**0.70 ± 0.04****	**1.51 ± 0.22***	1.42 ± 0.20	**3.70 ± 0.20*****

(Continued)

Table 2. (continued).

Metabolite	Wild-Type MG:*Psy*-1 MG	Wild-Type MG:Wild-Type Ripe	Wild-Type Ripe:*Psy*-1 Ripe	*Psy*-1 MG:*Psy*-1 Ripe
Polyols				
Erythritol	0.80 ± 0.07	**0.54 ± 0.02***	**1.80 ± 0.05*****	1.20 ± 0.06
Glycerol	0.60 ± 0.20	**0.20 ± 0.02****	**1.50 ± 0.13****	**0.40 ± 0.05****
Inositol	**0.31 ± 0.10****	**0.30 ± 0.03****	0.80 ± 0.07	0.80 ± 0.03
Mannitol	**1.70 ± 0.40***	**3.01 ± 0.12****	**2.54 ± 0.40****	**4.50 ± 0.60*****
Phosphates				
Fructose-6-phosphate	**0.49 ± 0.1***	**0.21 ± 0.02*****	**1.50 ± 0.13***	**0.30 ± 0.03****
Glucose-6-phosphate	**0.05 ± 0.005*****	**0.02 ± 0.00*****	1.40 ± 0.20	**0.57 ± 0.06****
Glycerol-3-phosphate	0.93 ± 0.10	**0.30 ± 0.06***	**1.60 ± 0.10****	**0.46 ± 0.07*****
Insitol-6-phosphate	**0.40 ± 0.02***	**0.40 ± 0.05****	**1.40 ± 0.07***	**1.40 ± 0.07*****
Phosphate	1.10 ± 0.09	**0.70 ± 0.05***	1.10 ± 0.05	**0.80 ± 0.03***
Sorbitol-6-phosphate	**0.34 ± 0.02*****	**0.23 ± 0.01*****	0.82 ± 0.03	**0.84 ± 0.02***
Sedoheptulose phosphate	**49.80 ± 2.50*****	**245.00 ± 39.00****	**16.10 ± 2.10*****	**7.80 ± 1.20*****
N-containing compounds				
Putrescine	0.94 ± 0.1	1.10 ± 0.15	**1.60 ± 0.13***	**0.50 ± 0.07****
Phenylpropanoids/flavonoids				
3-Caffeoylquinic	**0.40 ± 0.04*****	**0.33 ± 0.02****	**0.70 ± 0.06***	**0.60 ± 0.05*****
Chlorogenic acid	0.75 ± 0.04	**0.29 ± 0.18****	0.82 ± 0.03	**0.51 ± 0.02*****
Naringenin-chalcone	**0.23 ± 0.04****	**0.48 ± 0.03****	**0.25 ± 0.02****	**6.40 ± 0.30*****
Quercetin derivatives	1.25 ± 0.13	**0.35 ± 0.08****	**0.49 ± 0.03***	**1.32 ± 0.10***
Terpenoids				
Amyrin	1.14 ± 0.10	1.00 ± 0.01	1.14 ± 0.07	1.00 ± 0.01
Campesterol	0.96 ± 0.23	0.62 ± 0.90	1.06 ± 0.20	1.60 ± 0.20
α-Carotene	**~10.00#*****	**~10.00#*****	0.70 ± 0.10	1.60 ± 0.20
β-Carotene	**26.20 ± 2.80*****	**33.90 ± 1.20*****	1.40 ± 0.05	**1.81 ± 0.20*****
δ-Carotene	**~10.00#*****	**~10.00#*****	0.70 ± 0.10	1.60 ± 0.20
γ-Carotene	**~10.00#*****	**~10.00#*****	0.70 ± 0.03	1.60 ± 0.40
ζ-carotene	**~10.00#*****	**~10.00#*****	1.40 ± 0.10	1.20 ± 0.13
Cycloartenol	0.97 ± 0.26	1.20 ± 0.60	1.01 ± 0.05	1.10 ± 0.06
FPP[a]	0.78 ± 0.09	–	–	–
GGPP[a]	**0.10 ± 0.004****	–	–	–
GPP[a]	0.72 ± 0.2	–	–	–
Lutein	**2.40 ± 0.20***	1.10 ± 0.20	1.24 ± 0.10	**0.55 ± 0.03****
Lycopene	**~10.00#*****	**~10.00#*****	1.01 ± 0.06	**38.10 ± 2.20*****
Neoxanthin	1.20 ± 0.08	**0.20 ± 0.01*****	1.50 ± 0.10	**0.20 ± 0.01****
Phytoene	**~10.00#*****	**~10.00#*****	**2.30 ± 0.10****	**1.80 ± 0.20****
Phytofluene	**~10.00#*****	**~10.00#*****	**1.80 ± 0.10***	**1.80 ± 0.20***
Phytyl-PP[a]	**0.24 ± 0.025***	–	–	–
Sitosterol	1.09 ± 0.11	1.60 ± 0.31	0.70 ± 0.03	0.70 ± 0.14
Stigmasterol	0.87 ± 0.04	**3.12 ± 0.50****	0.99 ± 0.06	**2.90 ± 0.43****
α-Tocopherol	**2.40 ± 0.3****	**2.80 ± 0.60***	1.30 ± 0.20	1.30 ± 0.20
γ-Tocopherol	**~10.00#*****	**~10.00#*****	2.40 ± 1.30	**5.70 ± 2.50***
Ubiquinone	**0.12 ± 0.02****	**2.56 ± 0.50***	1.40 ± 0.30	**30.0 ± 3.00****
Violaxanthin	**1.30 ± 0.10**	**0.40 ± 0.03****	1.30 ± 0.04	**0.35 ± 0.02****
Zeaxanthin	1.30 ± 0.40	**0.50 ± 0.05***	2.20 ± 0.90	0.90 ± 0.40

The *Psy*-1 variety PS-1C26R2 (T_8) was used. Data have been normalized to sample weight and expressed relative to the wild type either at the mature green (37 d after anthesis) or ripe stage (10 d after breaker). In the case of column 5, data are expressed relative to the *Psy*-1 mature green samples. Values are represented as means ± SE, where $n = 6$. P values are shown as <0.0001, 0.001, and 0.05 by ***, **, and *, respectively. ~10.00# is at arbitrary increase due to the absence of one of a metabolite in one of the samples to be compared, while – indicates not determined. Terms in bold indicate a statistically significant increase. ND, not detected in one of the pairwise ratios; MG, mature green.

[a] Levels determined from radiolabeling experiments.

~80% changed significantly ($P < 0.05$) during fruit ripening. Glucose and fructose increased in ripe fruit, while sucrose and sugar phosphates decreased. Intermediates of the trichloroacetic acid (TCA) cycle were virtually all reduced. Cell wall–derived carbohydrates, organic acids, and sugars increased in content within the ripe fruit, as did the majority of polyols analyzed. All fatty acids analyzed were reduced in ripe fruit. With the exception of Lys, Asp, and Glu, amino acids decreased in ripe fruit compared with the mature green stage of fruit development. Among the isoprenoids, phytosterols and amyrin

contents were unchanged, but α-tocopherol levels increased. Changes in carotenoid and chlorophylls have been described in detail earlier.

Comparisons of the metabolites present in the *Psy*-1 mature green fruit with those in their wild-type comparators indicated that more than half (58%) of the metabolites had been altered in the *Psy*-1 fruit. Many of the changes correlated with those typically associated with the transition of green to red ripe fruit. For example, fatty acids and the majority of the TCA intermediates were decreased, as was the content of Lys, Asp, and Glu. Sucrose and sugar phosphates also decreased. In contrast with the metabolite changes associated with ripe fruit, the *Psy*-1 fruit at the mature green stage showed a reduced content of most cell wall–derived polysaccharides, while glucose and fructose were not altered.

In a similar manner to the metabolite changes associated with the transition of mature green to ripe fruit in the wild type, the *Psy*-1 variety also exhibited a very similar trend. Collectively, 73% of the metabolites were altered. Quantitative differences were apparent, for example, the decreases in fatty acids and glucose phosphate were not as significant, and cell wall–derived carbohydrates were greater than the changes associated with the wild-type transition from mature green to ripe. Metabolite analysis of ripe fruit from the wild type compared with the *Psy*-1 variety showed the least change in overall metabolites, although 43% of the metabolites were significantly altered. The most significant changes were elevations of amino acids and fatty acids (Figures 4 and 5).

Principal component analysis (PCA) was used to determine if the collective complement of metabolites was sufficiently different to distinguish wild-type and *Psy*-1 varieties as well as

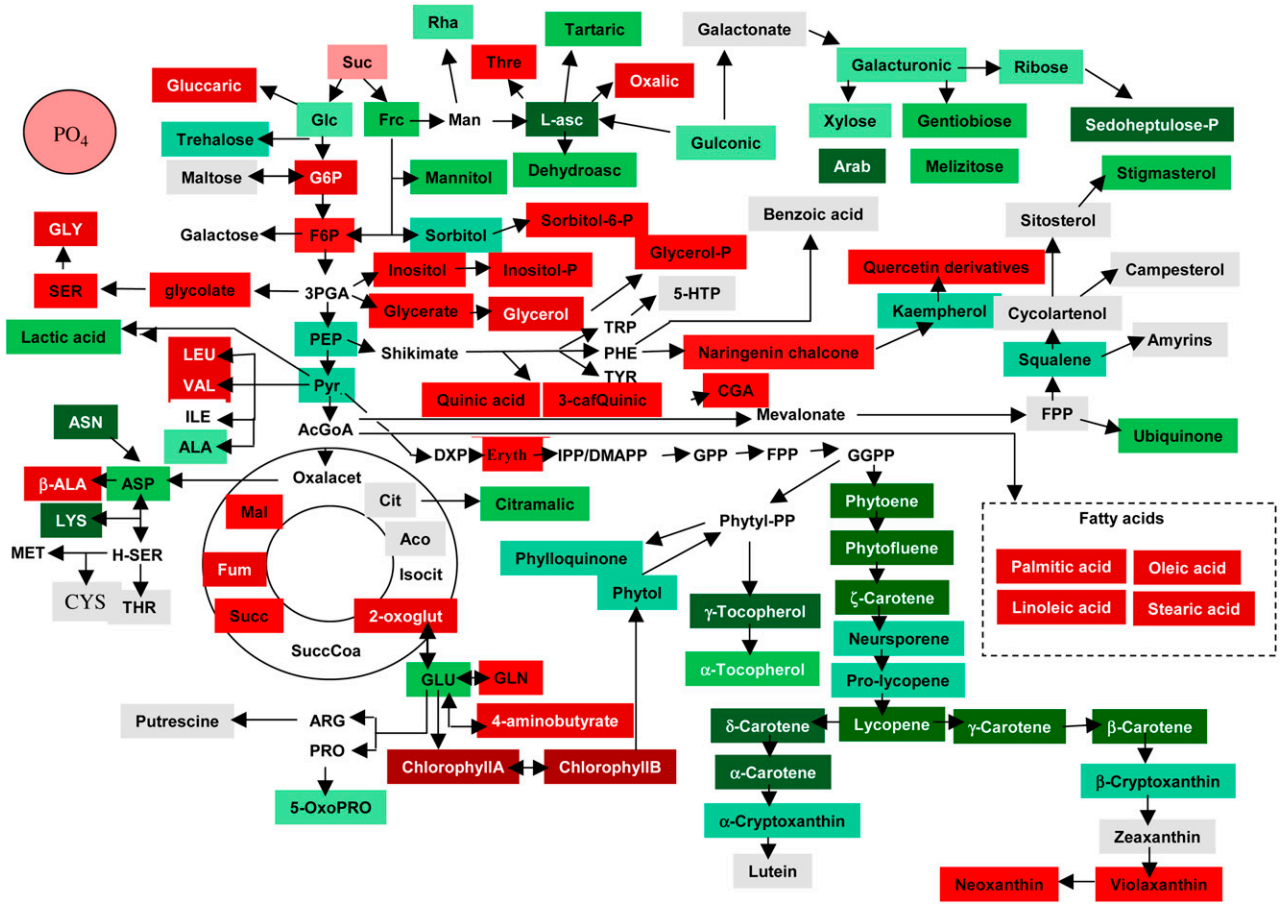

Figure 4. Metabolites Detected by Metabolomic Analysis and Displayed onto Schematic Representations of the Biochemical Pathways.

Changes arising from wild-type mature green fruit compared with wild-type ripe fruit. Data correspond to those displayed in Table 2. Green indicates an increased level of metabolite, with a significant to threefold increase in pale green, a threefold to eightfold increase in green, and more than eightfold is dark green. Gray indicates no significant change, while blue indicates that the metabolite was not detected in the samples. White indicates that the compound cannot be detected using the analytical parameters. Red coloration has been used to represent decreased metabolite levels; dark red is below eightfold, red is below twofold to fivefold, and pale red is below twofold. Aco, aconitic acid; L-Asc, ascorbic acid; citramal, citramalic acid; Cit, citric acid; dehydroasc, dehydroascorbic acid; Fum, fumaric acid; Mal, malic acid; 2-oxoglut, 2-oxoglutaric acid; Succ, succinic acid; Thre, threonic acid; 5HT, 5-hydroytryptamine; 5-OxoPRO, 5-oxo-proline; Arab, arabinose; DXP, deoxyxylulose-5-phosphate; F6P, fructose-6-phosphate; G6P, glucose-6-phosphate; 3-CaQuinic, 3-caffeoylquinic acid; CGA, chlorogenic acid; FPP, farnesyl diphosphate; GPP, geranyl diphosphate.

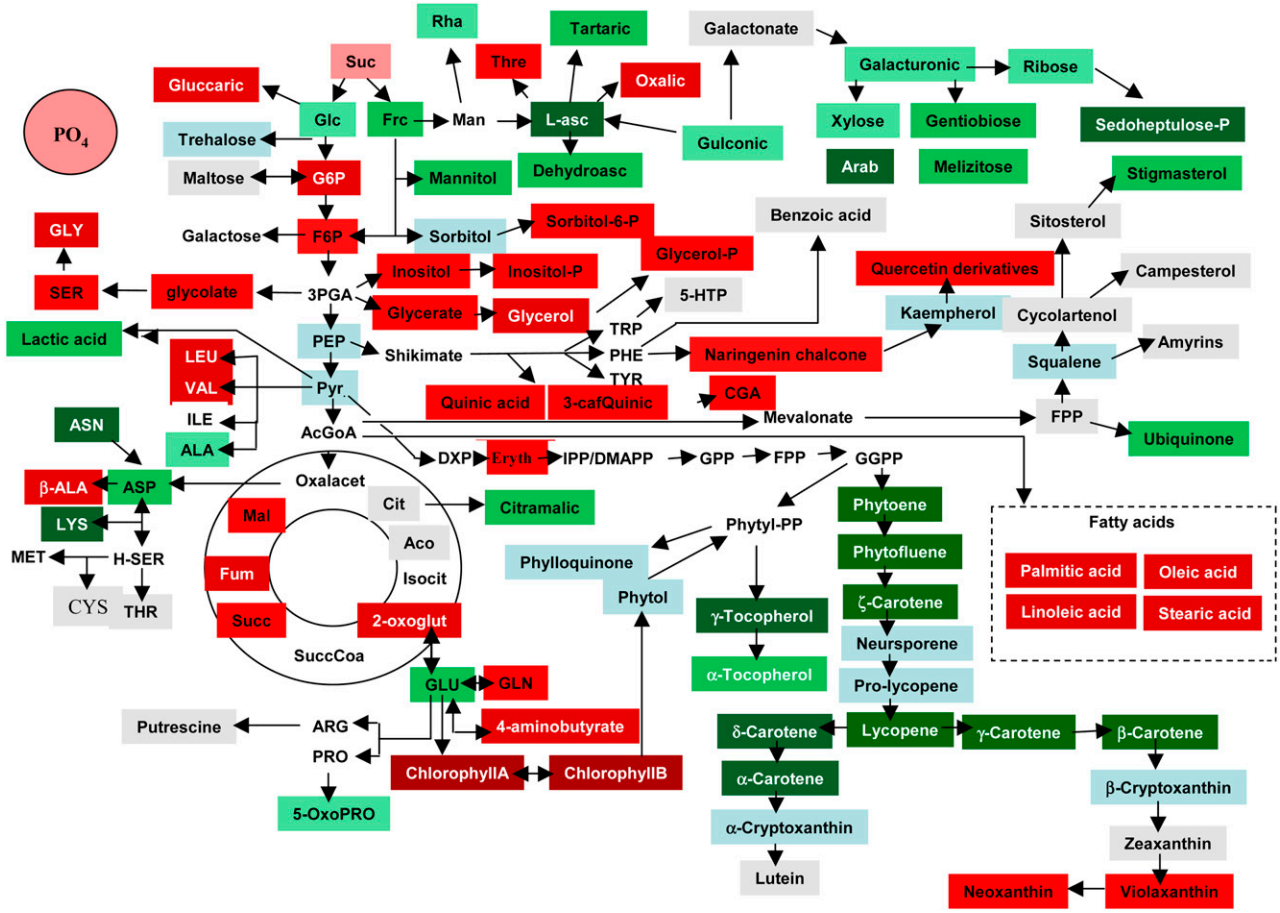

Figure 5. Metabolites Detected by Metabolomic Analysis and Displayed onto Schematic Representations of the Biochemical Pathways.

Changes arising from wild-type mature green fruit compared with *Psy*-1 mature green fruit. Abbreviations are the same as in Figure 4.

developmental and ripening stages of the fruit. All varieties and fruit stages form distinct clusters that can be separated principally in the direction of component 2 (Figure 6). The mature green fruit samples from the wild type and *Psy*-1 cluster closely to each other, with the ripe samples also clustering adjacent to each other. Intriguingly, the *Psy*-1 mature green cluster is closer to ripe fruit compared with the wild-type mature green fruit.

A Comparison of Fruit Development and Ripening Parameters in the *Psy*-1 Variety Compared with the Wild Type

To ascertain if the general parameters associated with fruit development and ripening had been affected as a result of constitutive *Psy*-1 expression, ethylene production, fruit firmness, pH, weight, and diameter were determined over fruit development and ripening. In addition, the length of time following pollination to reach specific fruit stages was determined (Figures 7A to 7F). Ethylene formation by detached fruit during development and ripening was virtually absent at the immature and mature green stages, followed by rapid synthesis at the breaker stage, which was maintained until 10 to 14 d after breaker. There was no significant difference between the wild-type and *Psy*-1 varieties. No significant changes in fruit firmness were found between the wild type and *Psy*-1. Similarly, fruit pH, days after pollination to reach specific developmental stages, and fruit weight and diameter all showed no significant differences between the two varieties.

DISCUSSION

A transgenic *Psy*-1–expressing tomato line, showing multiple inherited phenotypes up to at least the T6 generation, has been characterized in detail. The perturbations arising at the gene expression, enzyme activity, and the cellular and metabolomic levels can be primarily attributed to the manipulation of precursor/products used and formed by phytoene synthase, rather than the possibility of positional effects of transgene insertion site conferring the phenotype.

Increased Phytoene Synthesis Results in Feed-Forward Regulation of Carotenoid Formation in Tomato Fruit

Enhanced carotenoid accumulation in tomato fruit is normally coordinated with the onset of ripening at the breaker stage, as

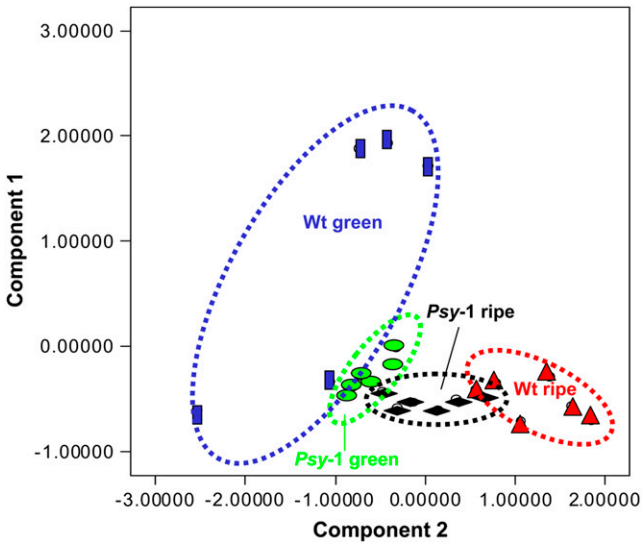

Figure 6. PCA of Metabolites Present in Wild-Type and *Psy*-1 Mature Green and Ripe Fruit.

Data analysis of the variables was performed as described in Methods. Components 1 and 2 were responsible for 40 and 16% of the total variance, respectively.

illustrated by the carotenoid changes in the wild-type fruit over development and ripening (Table 1). However, the *Psy*-1 transgenic variety does not exhibit the dramatic increase in pigmentation at the breaker stage, but at the mature green stage of fruit development (Table 1). Thus, it would appear that the accumulation of carotenoids in this variety is no longer associated with the coordinated process of fruit ripening. Determination of characteristic parameters associated with fruit development and ripening, such as ethylene production and firmness (Figure 6), confirmed that the progression of fruit ripening proceeds independently of carotenoid formation in this *Psy*-1 line and that analyses have been performed at comparable developmental stages.

The presence of phytoene at all developmental fruit stages is extremely rare and appears to trigger the coordinated synthesis of carotenoids. In effect, feed-forward regulation of the pathway has occurred. Previous reports describing the expression of a bacterial phytoene synthase in canola (*Brassica napus*) endosperm (Shewmaker et al., 1999) and rice (*Oryza sativa*) (Schaub et al., 2005) expressing a plant phytoene synthase and bacterial desaturase show enhanced synthesis of carotenoids beyond the point of manipulation. Determination of enzyme activities throughout the pathway indicated that phytoene synthase activity was elevated to the greatest extent (Figure 2B). Previous determinations of flux control coefficients indicated that phytoene synthase was the most influential step in the pathway (Fraser et al., 2002). Thus, the increase in PSY activity can account in part for the elevated level of carotenoids in green *Psy*-1 fruit. In addition, it illustrates that PSY-1, which is principally a ripening (chromoplast)-related phytoene synthase, functions in chloroplast-containing tissues. This contrasts with PSY-2, which does not contribute to flux control in ripe fruit (Fraser et al., 1999). Interestingly, *Psy*-2 expression was elevated in response to *Psy*-1 upregulation (Figure 2A). Presumably this is a response to increased phytoene synthase activity, altering GGPP precursor levels.

A correlation among *Cyc*-B gene expression, enzyme activity, and metabolite levels was found. Therefore, β-carotene formation from lycopene appears to be principally under transcriptional regulation, as described by Hirschberg (2001). By contrast, the lack of correlation between *Pds*, *Zds*, and *CrtISO* expression, enzyme activity, and especially metabolite levels suggests that posttranscriptional/translational regulation operates in these cases (Figure 2A).

In the Never-ripe (*Nr*) mutant, carotenoid formation is dependant on ethylene perception, which increases metabolic flux into the carotenoid pathway and restricts β-carotene formation (Alba et al., 2005). At the transcriptional level, *Psy*-1 was found to be independent of ethylene perception and not solely responsible for carotenoid pigmentation in fruit, while downregulation of the *Cyc*-B was ethylene dependent and responsible for lycopene accumulation. Our data do not support these findings because (1) carotenoid formation has been shown to be independent of ethylene perception, (2) phytoene synthase initiates pigment formation, and (3) carotenoid accumulation has arisen without *Cyc*-B downregulation. However, the two studies address different levels of regulation. In the *Nr* mutant, a more global regulation, via ethylene perception, is affected, whereas in the *Psy*-1 variety, an endogenous pathway is reacting to alterations in pathway precursor/product levels. An earlier study by Alba et al. (2000) established that phytochromes regulate light-induced lycopene accumulation independently of ethylene biosynthesis. Manipulation of precursor/products of the carotenoid pathway in mutants defective in ripening-related regulators is in progress to ascertain further regulatory mechanisms.

Perturbing Carotenoid Formation Affects Other Isoprenoids

Phytoene synthase expression has been linked to upregulation of early MEP biosynthetic genes (Lois et al., 2000; Rodriguez-Concepcion et al., 2001). This was also observed in this study for *Dxs* (Figure 2). However, instead of coordinated upregulation of *Psy*-1 and *Dxs*, the expression of the latter was reduced, though the enzyme activity was elevated. These data suggest that the early steps in isoprenoid formation react to changes in carotenoids, but the mechanisms of regulation are different at the gene and enzyme level. The occurrence of both transcriptional and posttranscriptional mechanisms operating in the MEP pathway has been reported (Sauret-Gueto et al., 2006).

Expression of the *Ggpps*-1 and 2 or resulting enzyme activities were not altered significantly in the *Psy*-1 lines (Figure 2). By contrast, incorporation of ^{14}C-IPP into GGPP showed a 90% reduction in the *Psy*-1 variety, while GPP and FPP were unaltered compared with the wild type. The concurrent premature depletion in chlorophyll with increased carotenoid formation in mature green fruit of the *Psy*-1 variety supports the view that GGPP is being preferentially used in the formation of carotenoids rather than chlorophyll. This suggests that the phytoene synthases alter the kinetics of the competing enzymes for GGPP. However,

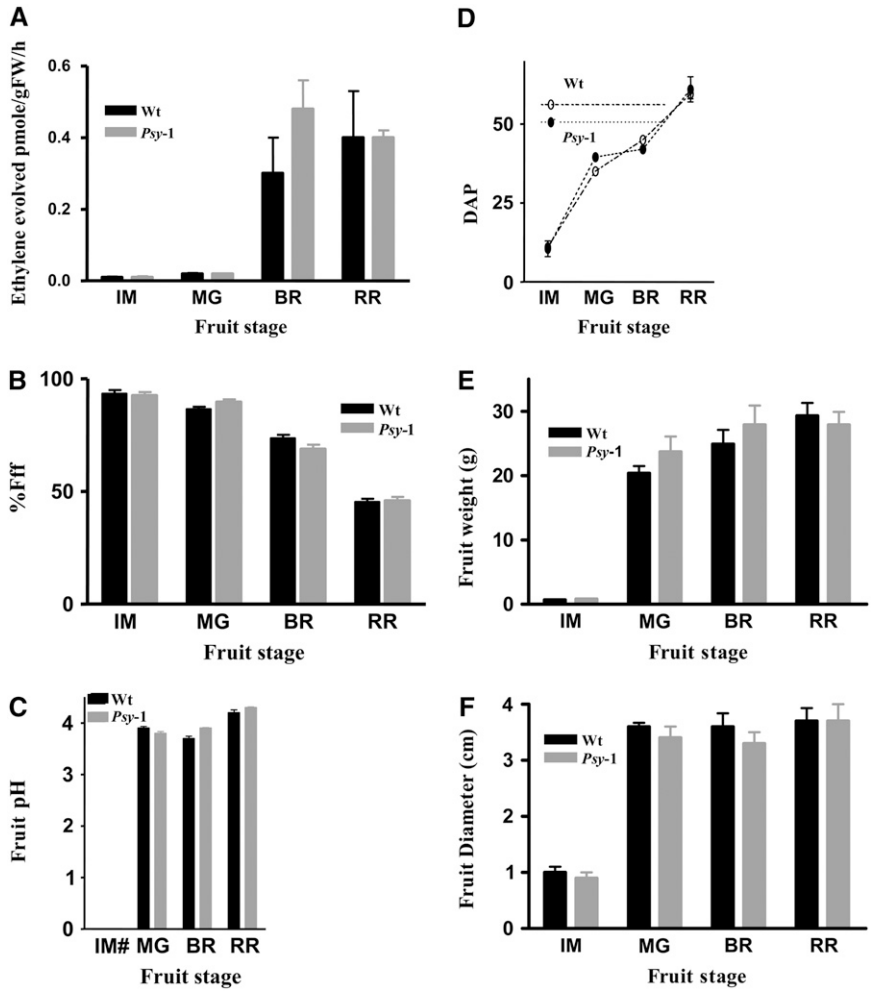

Figure 7. Comparison of General Ripening-Related Parameters Found in the Wild Type and *Psy*-1 Variety.

The *Psy*-1 variety PS-1C26R2 (T_{10}) was used for this analysis. Data sets have been represented as SE and statistical differences determined using Student's *t* test. IM, immature fruit; MG, mature green; BR, breaker; RR red ripe.

(A) Ethylene production of detached fruits. Three fruit at each stage were picked randomly from six plants, and three to four technical replications made.

(B) Determination of fruit firmness over fruit development and ripening. Four fruit were picked randomly from six plants and two to five technical replicates taken at the equator of each fruit.

(C) The pH of each fruit homogenate; three fruit were harvested randomly from six plants. Each fruit was quartered and a determination performed on four random quarters.

(D) The days after anthesis (DAP) required to reach observationally defined developmental and ripening stages. Typically, four determinations were made from flowers on the first three trusses.

(E) and **(F)** Fruit weight and diameter on four fruit from the same truss over development and ripening, for the immature, mature, and breaker stages. In the case of the ripe fruit, 22 wild-type fruit were used to determine the average fruit weight and 21 *Psy*-1 fruit used to determine the average fruit weight. Ripe fruit diameters were measured on four fruit.

tocopherol levels are elevated at this stage of fruit development in the *Psy*-1 variety compared with the wild type. Since all of these compounds use GGPP in their prenyl side chain, it is difficult to understand why one class of products increases (i.e., tocopherols) while chlorophyll decreases. One explanation proposed recently is that the phytyl chain necessary for tocopherol formation is derived from chlorophyll degradation (Ischebeck et al., 2006; Valentin, et al., 2006). From our study an extra 220 μmol of GGPP would be required to enable the increased synthesis of carotenoids, but only 8.5 μmol of GGPP to achieve the increased tocopherol levels, per tomato fruit. The reduction in chlorophyll would release 7 μmol of phytyl (i.e., GGPP equivalent). This suggests that chlorophyll degradation could be a source of GGPP for the synthesis of α-tocopherol in tomato fruit. However, this does not fully explain the premature degradation of chlorophyll. One explanation is that chlorophyll synthesis and degradation, as well as the phytyl salvage pathway, are active, but the increased channeling of GGPP into carotenoids depletes

chlorophyll synthesis, while degradation remains active and predominates over the phytyl salvage pathway to chlorophyll. In this way, the equilibrium between chlorophyll synthesis, degradation, and phytyl salvage is altered in favor of chlorophyll degradation and the resulting phytyl used in tocopherol synthesis. Despite its pivotal role in the formation of isoprenoids and the significant perturbations to isoprenoids derived from GGPP in the *Psy*-1 variety, *Ggpps*-1 and 2 expression and enzyme activities are very consistent, suggesting that early steps in the pathways derived from GGPP facilitate the redirection of common precursors.

The balance of carbon among interconnected branches of the isoprenoid pathway is clearly altered in the *Psy*-1 line mature green fruit. However, isoprenoids synthesized outside the plastid (i.e., phytosterols and ubiquinone) were unaffected. We could not detect an interaction between the two subcellular IPP-forming pathways. This finding concurs with previous reports that show that manipulating early isoprenoid pathway enzymes in both the mevalonate and MEP pathways has little effect on end-product isoprenoids from both pathways (Enfissi et al., 2005).

Metabolite-Induced Plastid Transition

There are numerous examples of plastid-localized transgenic proteins expressed in tomato fruit having no effect on plastid transition (e.g., Roemer et al., 2000). Therefore, it is unlikely that the increased activity of PSY-1 causes alterations in plastid type in mature green fruit (Figure 3). Instead, the changes are most likely the result of alterations in the metabolite composition in these fruit, especially carotenoids and chlorophylls. In the *Psy*-1–expressing fruit, the transition of chloroplasts into chromoplast-like structures occurs in a premature manner, and classical chromoplasts are not formed until the onset of ripening and carotenoid accumulation is advanced. Perhaps the absence of crystalline structures is because lycopene does not accumulate in these fruit. Instead, β-carotene, which is believed to reside in globules, is the most predominant carotenoid present. Changes in plastid morphology have been reported previously, resulting from elevated carotenoid levels in canola endosperm (Shewmaker et al., 1999). There is also evidence that morphological changes to cellular organelles can facilitate carotenoid accumulation. The cauliflower (*Brassica oleracea*) Orange gene product has been shown to trigger the transition of proplastids or other noncolored plastids into chromoplasts for carotenoid accumulation (Lu et al., 2006), and expression of fibrillin in tomato enhances accumulation of carotenoids (Simkin et al., 2007). Quantitative increases in plastid number have also been associated with elevated carotenoid pigmentation in the tomato high-pigment (*hp*-1) mutant (Liu et al., 2004).

Perturbations to *Psy*-1 Expression Cause Changes to the Metabolome

Relative changes in metabolites resulting from *Psy*-1 expression at the mature green developmental stage indicate that specific sectors of metabolism are altered (Table 2). These changes resemble metabolic changes associated with ripening (Carrari and Fernie, 2006) and indicate that the perturbations in carotenoid synthesis alter cellular metabolism and perhaps even physiological processes. Although the changes in the *Psy*-1 mature green fruit are similar to those found in ripening, the quantitative degree by which the metabolites alter is not as pronounced. In addition, several sectors of metabolism do not correlate with the changes associated with ripening. For example, elevation of cell wall–derived carbohydrates does not occur in the *Psy*-1 mature green fruit and probably explains why there are no observable effects on fruit softening (see Supplemental Table 1 online). There is no increase in Asp, a precursor of ethylene, in the *Psy*-1 variety at the mature green stage and also no elevation in ethylene production, while ripe fruit from the wild type and *Psy*-1 variety show an increase in Asp, correlating with ethylene production. Increased Glu in the mature green fruit of the *Psy*-1 variety, compared the wild type, is typical of a ripening-related transition.

Carrari et al. (2006) have shown coordinated shifts in segments of metabolism during fruit development and ripening. Similar correlations (e.g., organic acids of the TCA cycle with sugar phosphates) were observed in our study. However, Carrari et al. (2006) found that carotenoids showed the lowest number of significant correlations to other metabolites. In our study, considerable changes in the metabolite composition have been observed that reside from perturbed carotenoid formation. Other studies have also reported in situ manipulation of sucrose levels altering carotenoid formation (Télef et al., 2006). Presumably this illustrates the difference between systems that have been intentionally perturbed and unmodified physiological conditions.

PCA shows that *Psy*-1 mature green fruit cluster in the direction of those associated with ripe fruit rather than green wild-type fruit (Figure 6). Therefore, it would appear that the most pronounced effects on metabolism correlate with the greatest perturbations in carotenoid formation at the *Psy*-1 mature green stage. Although the *Psy*-1 variety shows significant changes in metabolite composition during fruit development, very limited pleiotropic effects arise. These findings illustrate that significant alterations to the chemotype can arise and emphasize the utility of fruit ripening–specific promoters for the control of transgene expression, thus reducing unintended effects. In conclusion, a detailed characterization of the *Psy*-1 transgenic variety has illustrated that manipulating phytoene synthase has far-reaching effects. The increase in phytoene synthase activity is the key driver to increased carotenoids. The changes in precursor/product ratios throughout the carotenoid pathway then alter gene expression within the pathway. Thus, gene expression responds to altered metabolite levels. Perturbations in carotenoid content and precursor pools appear to influence interconnected pathways and subsequently produce more global changes in the metabolome and plastid type. These effects arise without altering the general phenotype of the plant and fruit ripening. It would be interesting to see what effects these changes have on global gene expression. Potentially, inducible promoters could offer greater temporal and spatial control over events initiated by an additional *Psy*-1. Perhaps the use of different promoters with different expression profiles and potency would be an alternative, as reported by Davuluri et al. (2005).

METHODS

Generation and Preparation of Tomato Material

The wild-type tomato line used was *Solanum lycopersicum* Mill cv Ailsa Craig. Plants were glasshouse grown under supplementary lighting. Transformation was performed as described elsewhere (Bird et al., 1988) using *Agrobacterium tumefaciens* strain LBA 4404 and kanamycin resistance as a selection marker. The CaMV 35S promoter, present in a Bin 19–based vector (pJR1R), was used for constitutive expression. The entire open reading frame 1.5 kb of *Psy*-1 was placed downstream of the CaMV 35S. PCR analysis was performed using DNA extracted from young leaf material (200 mg) as described by Roemer et al. (2000). In brief, tissue was ground in a mortar and pestle under liquid nitrogen. Lysis buffer consisting of 1% hexadecyl trimethylammonium bromide, 0.2 M Tris-HCl, pH 7.5, 0.05 M EDTA, and 1 M NaCl was added (200 μL) and vortexed for 10 s. Then, 20 μL of sarcosyl (5%) was added to the suspension and left for 10 min at 65°C. Chloroform/isoamyl alcohol (600 μL; 24:1 v/v) was added and nucleic acids precipitated by adding an equal volume of isopropanol at −20°C. Samples were centrifuged at room temperature for 2 min at 9000*g*. The nucleic acid pellet was washed with 70% ethanol by volume, air dried, and washed again with 70% ethanol by volume. Finally, after repeated washing, the pellet was air dried and resuspended in 50 μL of 10 mM Tris and 1 mM EDTA, pH 7.4. PCR was performed using the following program: denaturation, 94°C for 0.8 min; annealing, 58°C for 0.2 min; extension, 72°C for 1.5 min; number of cycles, 30; final extension, 72°C for 6 min.

DNA for DNA gel blotting was extracted in accordance to Sambrook et al. (1989) and hybridization performed as described previously (Roemer et al., 2000; Fraser et al., 2002). Typically, leaf material from young plants was harvested and homogenized in 0.35 M sorbitol, 0.1 M Tris-HCL, pH 7.5, 0.005 M EDTA, and 0.02 M sodium metabisulphate. Genomic DNA (20 to 30 mg) was digested with *Eco*RI or *Hin*dII. Digested, genomic DNA fragments were separated on 0.8% agarose gels and then blotted onto membrane and hybridized at 65°C overnight. Blots were probed with a PCR-derived *npt*II fragment. Membranes were washed once with 5× SSC (0.15 M NaCl, 15 mM citric acid, and 0.2% SDS) at room temperature and then twice with 0.25× SSC, 0.2% SDS at 65°C before film exposure.

Kanamycin Germination Tests Were Performed with 30 Seeds on MS Agar Containing the Selection Marker at 50 μg/mL

Typically the same fruit material was used for metabolite and gene expression analyses. In these instances, three fruit were taken from three separate plants. Fruit were halved and deseeded. Pericarp tissue destined for metabolite analysis was frozen at −70°C and then lyophilized until completely dry. The dry material was milled into a fine homogeneous powder using a freezer-mill (Glen Creston) set at full power for 3 min. Intrasample variation was within 1% SE. Material to be used for gene expression analysis was homogenized using a freezer-mill under liquid nitrogen as described above. The powder was maintained in liquid nitrogen until frozen at −70°C for storage.

Measurement of Gene Expression by Quantitative Real-Time PCR

RNA was extracted from 100 to 200 mg of milled tissue using the RNeasy reagents and protocol (Qiagen), including on-column DNase digestion. The QuantiTect SYBR Green, one-step real-time RT-PCR kit (Qiagen) was used to determine gene expression levels. Per reaction, 25 ng of RNA was used and primers added to provided a final concentration of 0.3 μM in a final reaction volume of 20 μL. Reactions were performed on a Rotor-Gene 3000 thermocycler (Corbett Research). Thermocycling conditions were 30 min at 50°C for reverse transcription, 15 min at 95°C, followed by 30 to 40 cycles of 15 s at 94°C, 30 s at 56°C, and 30 s at 76°C. Sequencing of PCR products and melt curve analysis verified their specificity. For quantification, calibration curves were run simultaneously with experimental samples, and Ct calculations were performed by the Rotor-Gene software (Corbett Research). The actin gene served as reference for normalization.

Primers for quantitative real-time RT PCR were designed using *Primer3* software (http://primer3.sourcetorge.net/). The following primers for the PCR amplification were used: for *Dxs*, 5′-GCGGAGCTATTTCACATGGT-3′ (forward) and 5′-CTGCTGAGCATCCCAAT-3′ (reverse); *Ggpps*-1, 5′-GACAGCATCTGAGTCCGTCA-3′ (forward) and 5′-CTTGGCCAGGACAGAGTAGC-3′ (reverse); *Ggpps*-2, 5′-GGGATTGGAAAAGGCTAAGG-3′ (forward) and 5′-AGCAATCAATGGAGCAGCTT-3′ (reverse); *Psy*-1, 5′-TGGCCCAAACGCATCATATA-3′ (forward) and 5′-CACCATCGAGCATGTCAAATG-3′ (reverse); *Psy*-2, 5′-GTTGATGGCCCTAATGCATCA-3′ (forward) and 5′-TCAAGCATATCAAATGGCCG-3′ (reverse); *Pds*, 5′-GTGCATTTTGATCATCGCATTGAAC-3′ (forward) and 5′-GCAAAGTCTCTCAGGATTACCC-3′ (reverse); *Zds*, 5′-TTGGAGCGTTCGAGGCAAT-3′ (forward) and 5′-AGAAATCTGCATCTGGCGTATAGA-3′ (reverse); *CRTISO*, 5′-TTTTGGCGGAATCAACTACC-3′ (forward) and 5′-GAAAGCTTCACTCCCACAGC-3′ (reverse); *Lcy*-b, 5′-TCGTTGGAATCGGTGGTACAG-3′ (forward) and 5′-AGCTAGTGTCCTTGCCACCAT-3′ (reverse); *Cyc*-B, 5′-TGTTATTGAGGAAGAGAAATGTGTGAT-3′ (forward) and 5′-TCCCACCAATAGCCATAACATTTT-3′ (reverse); actin, 5′-AGGTATTGTGTTGGACTCTGGTGAT-3′ (forward) and 5′-ACGGAGAATGGCATGTGGAA-3′ (reverse).

Preparation of Subcellular Extracts from Tomato Fruit

Typically, three to four fruit at the 4 to 6 d after breaker stage were used to generate suitable cellular protein extracts as described previously (Fraser et al., 1994). The seeds were removed from the fruit and the pericarp tissue cut into small sections (1 to 2 cm^2). Subsequent procedures were performed at 4°C. Gentle homogenization was performed in a Waring blender full power for two 3-s bursts using ice-cold buffer (50 mM Tris-HCl, pH 8.0, containing 0.4 M sucrose and 1 mM DTT). The volume of buffer used was approximately three times the weight of the fruit material to be homogenized. The homogenate was filtered through four layers of cheesecloth and subsequently centrifuged at 9000*g* for 10 min. The supernatant was removed and the crude plastid pellet lysed osmotically in an equal volume of 0.4 M Tris-HCl, pH 8.0, containing 1 mM DTT. The mixture was homogenized in a handheld Potter homogenizer (three to five strokes) and then centrifuged at 105,000*g* for 1.5 h to yield a stromal (soluble) fraction and plastid membrane pellet (insoluble). The membrane fraction was resuspended in an equal volume (400 μL) of 0.4 M Tris-HCl, pH 8.0, containing 1 mM DTT.

Enzyme Assays

Enzyme activities within the plastid isoprenoid pathway and carotenoid biosynthesis were determined using radiolabeled substrates. Although the precise fruit tissues used to prepare extracts were not identical to that used for gene expression and metabolite analysis, the material did originate from the same growth cycle of plants. All activity values represent means and SE of three determinations, and values are expressed as dpm/mg protein/h, prior to creating a pairwise ratio with the appropriate control.

For DXS, incubation conditions, extraction, separation, and quantification of radiolabeled products formed during the determination of DXS activity have been described previously (Enfissi et al., 2005). The incubation buffer comprised 0.4 M Tris-HCl, pH 8.0, containing 1 mM DTT, 3 mM ATP, 2 μM $MgSO_4$, 2 μM $MnCl_2$, 1 mM KF, 0.1% Tween 60, 1 mM thiamine, and 4 μM D-glyceraldehyde-3-phosphate, with 0.25 μCi [2-^{14}C] pyruvate (30 mCi/mmol; ICN) as substrate, in a total volume of 200 μL. The reaction was initiated with the addition of the plastid fraction (200 μL). Incubations were shaken at 28°C for 3 h, after which the reaction was

terminated with acetone to a final concentration of 50% by volume. The solutions were mixed and stored at −20°C. Precursors and products were extracted by centrifugation at 3000*g* for 5 min to remove denatured protein and clarify the extract. The supernatant was removed, and aliquots of 5 to 10 μL applied to silica gel thin layers (silica gel 60; VWR) to separate precursors and reaction product. The mobile phase was isopropanol:ethyl acetate:water (6:1:3). Radioactive compounds were localized by autoradiography using x-ray Hyperfilm (VWR); typically, a 4-d exposure was required. Zones present on the thin layer chromatography (TLC) plates corresponding to radioactivity were scraped from the thin layers, and the radioactivity was determined by liquid scintillation counting. Cochromatographic behavior with authentic standards was used to identify deoxyxylulose (DX) and deoxyxylulose phosphate (DXP), having R_F values of 0.52 and 0.28, respectively. The DX and DXP standards were detected on TLC by staining with *p*-anisaldehyde/sulphuric acid (3:1); DX appears blue and DXP purple under these conditions.

For isopentenyl pyrophosphate isomerase (IPI), determination of IPI activity was performed in a similar manner to DXS except thiamine and D-glyceraldehyde-3-phosphate were omitted from the incubation buffer. The substrate used was 0.25 μCi [1-^{14}C-IPP] (56 mCi/mmol; purchased from Amersham) and activity determined using a stromal extract. After incubation, methanol (200 μL) was added, and acid hydrolysis was performed by treatment with concentrated HCl (25% final volume) for 1 h at 37°C, with shaking at 100 rpm. The prenyl alcohol derivatives were extracted with diethyl ether (500 μL × 2) and an aliquot (2% of the total volume) subjected to liquid scintillation counting to determine the radioactivity incorporated.

For GGPP synthase, identical incubation conditions and product analysis as to those used for IPI were performed to ascertain GGPP synthase activity, with the exception that in addition to ^{14}C-IPP as substrate, dimethylallyl diphosphate was added to a final concentration of 2 mM from a 200 mM stock prepared in methanol.

For PSY, 0.5 μCi [^{3}H]GGPP, (15 mCi/mmol; American Radiolabeled Chemicals) was used as the substrate to determine PSY activity. Stromal extracts (200 μL) were used in the assay, and the buffered cofactor mixture was the same as that used for IPI. Incubations were performed for 3 h at 25°C and shaken at 100 rpm. The reaction was terminated with the addition of methanol (200 μL). The incubation mixture was either stored at −20°C or extracted. Phytoene and other nonpolar components were extracted with chloroform (500 μL). After mixing, the suspension was centrifuged at 3000*g* for 3 min to create a partition. The organic hypophase was removed and the remaining aqueous phase reextracted with chloroform (500 μL). The organic phases were combined and reduced to dryness under a stream of nitrogen. The reaction products were analyzed by TLC (Fraser et al., 1991) and confirmed by radio-HPLC (Fraser et al., 1993). Authentic phytoene was prepared as described previously (Fraser et al., 1991). The TLC system used activated aluminum oxide (VWR) with a mobile phase of 6% toluene in petroleum ether at 40 to 60°C. The dried organic extract from the in vitro assay was resuspended in ethyl acetate (20 μL), containing 1 μg of phytoene standard and applied to the TLC plate. After 1 h, the plate was air dried and stained with iodine to locate phytoene (R_F of 0.65 to 0.68). After staining, the zone was scraped off, the gel added to scintillation fluid, and the radioactivity analyzed (Bramley et al., 1973).

For PDS, a coupled assay procedure was used as described previously (Fraser et al., 1991, 1994) to determine desaturation of phytoene by membrane fractions of tomato plastids. This method uses the ability of a cell extract from the *Phycomyces blakesleeanus* C5 *car*B to produce ^{14}C-phytoene in situ from ^{14}C-IPP. The cultivation of *P. blakesleeanus* is described by Than et al. (1972). Mycelia were harvested by filtration through cheesecloth (two layers) and lyophilizing to complete dryness. The cell extract was prepared by rubbing the mycelia through a 180-μm mesh sieve and then the fine powder cold buffer (0.4 M Tris-HCl, pH 8.0, containing 1 mM DTT) was added at a ratio of 1:5 by weight. The paste was thoroughly stirred and centrifuged at 9000*g* for 20 min at 4°C. The resulting supernatant was removed and then centrifuged at 105,000*g* for 1 h. The clarified extract (200 μL) was used to generate ^{14}C-phytoene. The cofactor mixture contained $MgCl_2$ (5 mM), $MnCl_2$ (3 mM), Tween 60 (0.1%), NAD, NADP, NADPH, FAD (1.5 mM), decyl-plastoquinone (10 μM), ATP (5 mM), and 0.5μCi [1-^{14}C-IPP] (56 mCi/mmol; purchased from Amersham) buffered in 0.4 M Tris-HCl, pH 8.0, containing 1 mM DTT to a final volume of 100 μL. The tomato plastid membrane suspension (200 μL) was added and the solutions mixed and incubated for 5 h at 25°C, with shaking at 100 rpm. The reaction was terminated with methanol (500 μL) and extracted with chloroform (1 mL) twice and the pooled extracts dried under nitrogen. The dried extract was dissolved in ethyl acetate (20 μL) containing authentic phytoene, phytofluene, ζ-carotene, and β-carotene (each 1 μg), applied to silica gel TLC (VWR) and chromatographed in 15% toluene in petroleum ether at 40 to 60°C. Lycopene (R_F 0.4) was scraped off, scintillation fluid added, and radioactivity assayed. ζ-Carotene, phytofluene, β-carotene, and phytoene migrated within R_F values of 0.5 to 0.8. This section was removed, eluted from the silica, and rechromatographed on activated aluminum oxide (VWR) with a solvent mixture of 3% toluene in petroleum ether at 40 to 60°C. ζ-Carotene (R_F 0.30) and β-carotene (R_F 0.5) were visualized from their color. Phytoene (R_F 0.7) and phytofluene (R_F 0.6) were visualized with iodine vapor. Bands were scraped off and radioactivity quantified by liquid scintillation counting (Bramley et al., 1973).

For lycopene cyclization, ^{14}C-lycopene was produced in situ using a crude extract prepared from *P. blakesleeanus* C9 *car*RA mutant. The ability of plastid-derived membranes to metabolize the lycopene was determined using a procedure identical to that used for phytoene desaturation and is described elsewhere (Fraser et al., 1994).

For analysis of products derived from ^{14}C-IPP, determination of products formed from ^{14}C-IPP was achieved by extending the incubation period to 5 h. Nonpolar radiolabeled reaction products were extracted from the incubation mixture by partitioning with chloroform (500 μL × 2). The remaining aqueous phase was treated with concentrated HCl (25% final concentration). Following incubation for 1 h at 37°C, the prenyl alcohols were extracted as described above for the IPI assay, with the exception that a standard prenyl alcohol mixture (equivalent to 1 μg per prenyl alcohol dissolved in petroleum ether at 40 to 60°C) was added to facilitate identification on subsequent TLC separations. The prenyl alcohols were separated by reverse-phase C_{18} silica TLC (VWR) developed in methanol:water (95:5). The R_F values were 0.82, 0.61, 0.45, 0.32, and 0.19 for dimethylallyl alcohol, geraniol, farnesol, geranylgeranyl alcohol, and phytol, respectively. These compounds were detected by staining with iodine. The stained zones corresponding to prenyl alcohols were scraped off and the gel added to scintillation fluid prior to counting. Phytoene was determined as described above using the PSY assay.

Metabolite Analysis

Carotenoid and Isoprenoid Analysis

The extraction, HPLC separation, photodiode array detection, and quantification of carotenes, carotenoids, xanthophylls, tocopherols, and quinones have been described in detail previously (Fraser et al., 2000). A 10- to 20-mg aliquot of ground homogeneous fruit tissue was extracted with chloroform and methanol (2.5:1 by volume), stored for 20 min on ice, and 1 volume of 100 mM Tris-HCl, pH 8.0, added. The organic hypophase was removed and the aqueous phase reextracted with chloroform (2.5 by volume). The pooled extracts were dried under nitrogen gas. The residue was resuspended in ethyl acetate (50 μL). HPLC separations were performed using a C_{30} reverse-phase column (250 × 4.6 mm) purchased from YMC. The mobile phases used were methanol (A), water/methanol (20/80 by volume), containing 0.2% ammonium acetate (B), and *tert*-methyl butyl ether (C). The gradient was 95% A:5%B, isocratically for 12 min, stepped to 80% A:5%B:15%C, from which a linear gradient to

30%A:5%B:65%C over 30 min was performed. A Waters Alliance model 2695 injection and solvent delivery system was used. Detection was performed continuously from 220 to 700 nm with an online photodiode array detector (Waters 966). Identification was performed by cochromatography and comparison of spectral properties with authentic standards and reference spectra (Britton et al., 2004). Quantitative determination of carotenoids was performed by comparison with dose–response curves (0.2 to 1.0 μg) constructed from authentic standards. Purchasing, preparation, and characterization of standards have been described previously (Fraser et al., 2000; Long et al., 2006). To assist identification in some cases, mass spectra of the carotenoids were acquired using off-line matrix-assisted laser-desorption ionization time of flight/mass spectrometry (Bruker Reflex III; Bruker Daltonics) as described elsewhere (Fraser et al., 2007).

Flavonoid and Phenylpropanoid Analysis

Procedures used to extract, separate, detect, and quantify phenylpropanoids and flavonoids from lyophilized tomato material have been detailed previously (Davuluri et al., 2005; Long et al., 2006). Typically, 20 mg of freeze-dried powder (homogenized in the freezer mill as described earlier) was extracted with methanol (1 mL). Salicylic acid was also added to this suspension as an internal standard (10 μg). The mixture was heated to 90°C for 60 min in a Pyrex test tube then placed on ice until cool. The samples were then centrifuged at 3000*g* for 5 min, the supernatant removed, and extracts passed through a 0.2-μm filter before HPLC analysis. A Dionex Gynkotek HPLC solvent delivery system was used to separate phenylpropanoids and flavonoids on a reverse-phase C_{18} column (250 × 4.6-mm; 5 μm; Hichrom). The mobile phase consisted of (A) 2% water in methanol acidified with 0.015% HCl by volume and (B) acetonitrile. The initial gradient conditions used were 95% A and 5% B for 10 min, followed by a linear gradient to 50% B over 30 min. An online photodiode array detector enabled detection and identification from characteristic UV/Vis spectra. Authentic standards were used to confirm the identity of the phenylpropanoids and flavonoids. Relative quantification was performed by comparison of integrated peak areas with the internal standard at the maximum wavelength of the phenylpropanoids and flavonoids detected.

Phytosterol Analysis

Total phytosterols were routinely extracted from ground tomato powder prepared in the freezer mill as described above. β-Cholestanol was added as an internal standard (20 μg) and the suspension saponified with 5% KOH in 80% ethanol (5 mL) for 1 h at 90°C. When cooled, this solution was neutralized with concentrated sulphuric acid (~200 μL). The phytosterols were extracted with hexane (2 × 3 mL), adding water (5 mL) to create a partition. The pooled hexane extracts were dried under nitrogen and the residue redissolved in acetonitrile (20 μL) and derivatized by adding 20 μL of *N*-methyltrimethylsilytrifluoroacetaminde (MSTFA; Sigma-Aldrich). This mixture was incubated at 37°C for 1 h. Separation and detection of phytosterols was performed with a Varian CP3380 gas chromatograph, containing a flame ionization detector and autosampler CP8410. Separation was on a CP-SIL8 column (Varian). The temperature program consisted of 140°C initial conditions increasing to 240°C by 27 min at 4°C per min holding for 2 min. These conditions were then held for another 18 min. The injector (Varian 1177) temperature was set at 260°C. Quantification was performed from integrated peak areas relative to a known amount of the internal standard.

Extraction, Derivatization, and Gas Chromatography–Mass Spectrometry Analysis of Metabolites

To an aliquot (20 to 25 mg) from the freezer milled tomato powder the internal standards (20 μL), ^{13}C benzoic acid (20 mg/mL), and ^{13}C ribitol (20 mg/mL) were added. Methanol (1 mL; HPLC grade) was placed onto the material and the suspension mixed vigorously and then incubated at room temperature for 30 min with continuous agitation. To remove cell debris, samples were centrifuged at 12,000 rpm for 2 min. The resulting supernatant was removed and from each sample an aliquot (100 μL) dried under nitrogen gas. At this point, the extracts could be derivatized immediately or stored without degradation at −20°C. Derivatization was performed by the addition of 30 μL of methoxyamine-HCl (Sigma-Aldrich), prepared at a concentration of 20 mg/mL in pyridine. After incubation in screw-capped tubes at 37°C for 2 h, MSTFA was added (85 μL) and the samples incubated for a further 1 h at 37°C before analysis. Gas chromatography–mass spectrometry (GC-MS) analysis was performed on an Agilent HP6890 GC with a 5973MSD. Typically, samples (1 μL) were injected with a split/splitless injector at 290°C with a 20:1 split. Retention time locking to the internal standard was used. The GC oven was held for 4 min at 70°C before ramping at 5°C/min to 310°C. This final temperature was held for a further 10 min, making a total time of 60 min. The interface with the MS was set at 290°C and MS performed in full scan mode using 70 eV EI+ and scanned from 10 to 800 D. To identify chromatogram components found in the tomato profiles, an MS library was constructed from in-house standards and the NIST 98 mass spectral library. The automated mass spectral deconvolution and identification system initially processed chromatogram components. A retention time calibration was performed on all standards to facilitate the determination of retention indices. Using the retention indices and MS, identification was performed by comparison with the MS library. Quantification was achieved using Chemstation software (Agilent), facilitating integrated peak areas for specific compound targets (qualifier ions) relative to the ribitol internal standard peak.

Determination of Fruit Developmental and Ripening Parameters

Fruit Firmness

The firmness of fruit was determined using a firmness meter, fitted with a 0.25-cm^2 probe, as recommended for tomato (Qualitest; www.worldoftest.com). Typically, 10 readings were performed around the equator of the fruit.

Ethylene Determinations

Fruit at defined stages of development and ripening were placed in gas-tight jars (one fruit per jar) containing a self-sealing septum in the lid. After incubation at room temperature for 12 h, a sample of the gas was taken (4 mL). Using a Varian CP3380 gas chromatogram connected to a flame ionization detector, ethylene was determined by injecting 1 mL of the head space gas directly in a splitless mode. The injector temperature was set at 70°C and the oven temperature 40°C. Separation was performed on a CP-PoraPLOT Q column (Varian). Ethylene was identified on the chromatogram by cochromatography with an authentic standard. To quantify the ethylene peaks, a dose–response curve was created by injecting known concentrations from a 5 ppm standard (CryoService). The ethylene evolved is presented as pmole/h/g fresh weight.

Fruit pH

From three different fruits, four representative quarters were homogenized with an Ultra Turrax (VWR) for three 20-s bursts. A pH electrode was then placed into the resulting homogenate and the pH recorded.

Statistical Treatment of Data

Metabolites levels from the multitechnology platforms were combined and used as variables, on which PCA was performed. SPSS software, version 12.01, was used to display clusters derived from PCA. Student's *t* tests were used to determine significant differences between pairwise comparison of the wild type and the transgenic variety. Student's *t* tests, means, and SE were calculated using GraphPad Prism software. The

layout for overlaying biochemical pathways was modified from that of Carrari and Fernie (2006).

Other Determinations

Protein levels were estimated as described by Bradford (1976).

Accession Numbers

Sequence data for the tomato genes used can be found in the GenBank/EMBL data libraries under the following accession numbers. *Dxs*, AF143812; *Ggps*1, U215952; *Ggps*2, SGN-U223568; *Psy*-1, Y00521; *Psy*-2, L23424; *Pds*, X59948; *Zds*, AF195507; *Actin*, BT013524; *CRTISO*, AF416727; *Lcy*-b, X86452; and *CYC*-B, AF254793.

Supplemental Data

The following materials are available in the online version of this article.

Supplemental Figure 1. Overview of Isoprenoid Formation in Higher Plants.

Supplemental Figure 2. Carotenoid Biosynthesis in Vegetative and Ripe Tissues of Tomato.

Supplemental Figure 3. Metabolites Detected by Metabolomic Analysis, Displayed onto Schematic Representations of the Biochemical Pathways, Showing Changes Arising from Wild-Type Fruit Compared with *Psy*-1 Ripe Fruit.

Supplemental Figure 4. Metabolites Detected by Metabolomic Analysis, Displayed onto Schematic Representations of the Biochemical Pathways, Showing Changes Arising from *Psy*-1 Mature Green Fruit Compared with *Psy*-1 Ripe Fruit.

Supplemental Table 1. Color Phenotypes and Total Carotenoid Content of Mature Green and Ripe Fruit from Transgenic Plants Containing an Additional *Psy*-1 Compared with Wild-Type (Ailsa Craig) Controls.

Supplemental Table 2. General Phenotypic Properties of the *Psy*-1 Variety Compared with Wild-Type Plants.

Supplemental Table 3. Analysis of Carotenoid/Isoprenoid Profiles Found in Mature Green Fruit from the Wild Type (Ailsa Craig) and *Psy*-1 Tomato Fruit.

Supplemental Table 4. Analysis of Carotenoid/Isoprenoid Profiles Found in Ripe Fruit from the Wild Type (Ailsa Craig) and *Psy*-1 Tomato Fruit.

ACKNOWLEDGMENTS

This work was supported in part by European Union Framework IV (ProVitA QLK3-CT2000-0809). We thank Syngenta for cultivation of some of the tomato crops and for a Cooperative Award in Science and Engineering to M.R.T. with the Biotechnology and Biological Science Research Council. We also thank Tadhg Begley (Cornell University, Ithaca, NY) for the provision of 1-deoxy-D-xylulose-5-phosphate and B. Camara (University of Strasbourg, Germany) for 1-deoxy-D-xylulose.

Received December 20, 2006; revised August 31, 2007; accepted September 12, 2007; published October 12, 2007.

REFERENCES

Alba, R., Cordonnier-Pratt, M.-M., and Pratt, L.H. (2000). Fruit-localized phytochromes regulate lycopene accumulation independently of ethylene production in tomato. Plant Physiol. **123:** 363–370.

Alba, R., Payton, P., Fei, Z., McQuinn, R., Debbie, P., Martin, G., Tanksley, S.D., and Giovannoni, J.J. (2005). Transcriptome and selected metabolite analyses reveal multiple points of ethylene control during tomato fruit development. Plant Cell **17:** 2954–2965.

Alexander, L., and Grierson, D. (2002). Ethylene biosynthesis and action in tomato: A model for climacteric fruit ripening. J. Exp. Bot. **53:** 2039–2055.

Bird, C.R., Smith, C.J.S., Ray, J.A., Moreau, P., Bevan, M.W., Bird, A.S., Hughes, S., Morris, P.C., Grierson, D., and Schuch, W. (1988). The tomato polygalacturonase gene and ripening-specific expression in transgenic plants. Plant Mol. Biol. **11:** 651–662.

Booker, J., Auldridge, M., Wills, S., McCarty, D., Klee, H., and Leyser, C. (2004). MAX3/CCD7 is a carotenoid cleavage dioxygenase required for the synthesis of a novel plant signalling molecule. Curr. Biol. **14:** 1232–1238.

Bradford, M.M. (1976). A rapid and sensitive method for the quantitation of microgram quantities of protein utilizing the principle of protein-dye binding. Anal. Biochem. **72:** 248–254.

Bramley, P.M., Davies, B.H., and Rees, A.F. (1973). Colour quenching by carotenoids. In Liquid Scintillation Counting, Vol. 3, M.A. Crook and P. Johnson, eds (London: Heyden), pp. 67–85.

Britton, G., Liaaen-Jensen, S., and Pfander, H., eds (2004). Carotenoids Handbook. (Basel, Switzerland: Birkhauser Verlag).

Carrari, F., Baxter, C., Usadel, B., Urbanczyk-Wochniak, E., Zanor, M.-I., Nunes-Nesi, A., Nikiforova, V., Centero, D., Ratzka, A., Pauly, M., Sweetlove, L.J., and Fernie, A. (2006). Integrated analysis of metabolite and transcript levels reveals the metabolic shifts that underlie tomato fruit development and highlight regulatory aspects of metabolic network behaviour. Plant Physiol. **142:** 1380–1396.

Carrari, F., and Fernie, A.R. (2006). Metabolic regulation underlying tomato fruit development. J. Exp. Bot. **57:** 1883–1897.

Cunningham, F.X., Jr., and Gantt, E. (2001). One ring or two? Determination of ring number in carotenoids by lycopene epsilon-cyclases. Proc. Natl. Acad. Sci. USA **98:** 2908–2910.

Davuluri, G.R., et al. (2005). Fruit-specific RNAi-mediated suppression of *DET1* enhances tomato nutritional quality. Nat. Biotechnol. **23:** 890–895.

DellaPenna, D., and Pogson, B. (2006). Vitamin synthesis in plants: Tocopherols and carotenoids. Annu. Rev. Plant Biol. **57:** 11–38.

Demmig-Adams, B., and Adams III, W.W. (2002). Antioxidants in photosynthesis and human nutrition. Science **298:** 2149–2153.

Enfissi, E.M.A., Fraser, P.D., Lois, L.M., Boronat, A., Schuch, W., and Bramley, P.M. (2005). Metabolic engineering of the mevalonate and non-mevalonate isopentenyl diphosphate-forming pathways for the production of health-promoting isoprenoids. Plant Biotechnol. J. **2:** 17–27.

Fiore, A., Dall'Osto, L., Fraser, P.D., Bassi, R., and Giuliano, G. (2006). Elucidation of the β-carotene hydroxylation pathway in *Arabidopsis thaliana*. FEBS Lett. **580:** 4718–4722.

Fraser, P.D., Albrecht, M., and Sandmann, G. (1993). Development of high-performance liquid chromatographic systems for the separation of radiolabelled carotenes and precursors formed in specific enzymatic reactions. J. Chromatogr. **645:** 265–272.

Fraser, P.D., and Bramley, P.M. (2004). The biosynthesis and nutritional uses of carotenoids. Prog. Lipid Res. **43:** 228–265.

Fraser, P.D., De Las Rivas, J., Mackenzie, A., and Bramley, P.M. (1991). *Phycomyces blakesleaanus* CARB mutants-Their use in assays of phytoene desaturase. Phytochemistry **30:** 3971–3976.

Fraser, P.D., Enfissi, E.M.A., Goodfellow, M., Eguchi, T., and Bramley, P.M. (2007). Metabolite profiling of plant carotenoids using matrix assisted laser desorption ionisation time of flight mass spectrometry. Plant J. **49:** 552–564.

Fraser, P.D., Kiano, J.W., Truesdale, M.R., Schuch, W., and Bramley, P.M. (1999). Phytoene synthase-2 enzyme activity in tomato does not contribute to carotenoid synthesis in ripening fruit. Plant Mol. Biol. **40:** 687–698.

Fraser, P.D., Pinto, M.E.S., Holloway, D.E., and Bramley, P.M. (2000). Application of high-performance liquid chromatography with photodiode array detection to the metabolic profiling of plant isoprenoids. Plant J. **24:** 551–558.

Fraser, P.D., Roemer, S., Shipton, C.A., Mills, P.B., Kiano, J.W., Misawa, N., Drake, R.G., Schuch, W., and Bramley, P.M. (2002). Evaluation of transgenic tomato plants expressing an additional phytoene synthase in a fruit-specific manner. Proc. Natl. Acad. Sci. USA **99:** 1092–1097.

Fraser, P.D., Truesdale, M.R., Bird, C.R., Schuch, W., and Bramley, P.M. (1994). Carotenoid biosynthesis during tomato fruit development: Evidence for tissue-specific gene expression. Plant Physiol. **105:** 405–413.

Fray, R.G., Wallace, A., Fraser, P.D., Valero, D., Hedden, P., Bramley, P.M., and Grierson, D. (1995). Constitutive expression of a fruit phytoene synthase gene in transgenic tomatoes causes dwarfism by redirecting metabolites from the gibberellin pathway. Plant J. **8:** 693–701.

Giovannoni, J.J. (2004). Genetic regulation of fruit development and ripening. Plant Cell **16:** S170–S180.

Giovannucci, E. (2002). Lycopene and prostate cancer risk. Methodological considerations in the epidemiologic literature. Pure Appl. Chem. **74:** 1427–1434.

Hirschberg, J. (2001). Carotenoid biosynthesis in flowering plants. Curr. Opin. Plant Biol. **4:** 210–218.

Isaacson, T., Ohad, I., Beyer, P., and Hirschberg, J. (2004). Analysis in vitro of the enzyme CRTISO establishes a poly-cis-carotenoid biosynthesis pathway in plants. Plant Physiol. **136:** 4246–4255.

Isaacson, T., Ronen, G., Zamir, D., and Hirschberg, J. (2002). Cloning of tangerine from tomato reveals a carotenoid isomerase essential for the production of beta-carotene and xanthophylls in plants. Plant Cell **14:** 333–342.

Ischebeck, T., Zbierzak, A.M., Kanwischer, M., and Dormann, P. (2006). A salvage pathway for phytol metabolism in *Arabidopsis*. J. Biol. Chem. **281:** 2470–2477.

Kim, J., and DellaPenna, D. (2006). Defining the primary route for lutein synthesis in plants: the role of *Arabidopsis* carotenoid β-ring hydroxylase CYP97A3. Proc. Natl. Acad. Sci. USA **103:** 3474–3479.

Landrum, J.T., and Bone, A.R. (2001). Lutein, zeaxanthin, and the macular pigment. Arch. Biochem. Biophys. **385:** 28–40.

Liu, Y., Roof, S., Ye, Z., Barry, C., van Tuinen, A., Verbalov, J., Bowler, C., and Giovannoni, J. (2004). Manipulation of light signal transduction as a means of modifying fruit nutritional quality in tomato. Proc. Natl. Acad. Sci. USA **101:** 9897–9902.

Lois, L.M., Rodriguez-Concepcion, M., Gallego, F., Campos, N., and Boronat, A. (2000). Carotenoid biosynthesis during tomato fruit development: Regulatory role of 1-deoxy-D-xylulose 5-phosphate synthase. Plant J. **22:** 503–513.

Long, M., Millar, D.J., Kimura, Y., Donovan, G., Rees, J., Fraser, P.D., Bramley, P.M., and Bolwell, G.P. (2006). Metabolite profiling of carotenoid and phenolic pathways in mutant and transgenic lines of tomato: Identification of a high antioxidant fruit line. Phytochemistry **67:** 1750–1757.

Lu, S., et al. (2006). The cauliflower *Or* gene encodes a DnaJ cysteine-rich domain-containing protein that mediates high levels of β-carotene accumulation. Plant Cell **18:** 3594–3605.

Mayne, S.T. (1996). β-Carotene, carotenoids and disease prevention in humans. FASEB J. **10:** 690–701.

Picton, S., Gray, J., Barton, S., AbuBakar, U., Lowe, A., and Grierson, D. (1993). cDNA cloning and characterisation of novel ripening-related mRNAs with altered patterns of accumulation in the ripening inhibitor (rin) tomato ripening mutant. Plant Mol. Biol. **23:** 193–207.

Rodriguez-Concepcion, M., Ahumada, I., Diez-Juez, E., Sauret-Gueto, S., Lois, L.M., Gallego, F., Carretero-Paulet, L., Campos, N., and Boronat, A. (2001). 1-Deoxy-D-xylulose 5-phosphate reductoisomerase and plastid isoprenoid biosynthesis during tomato fruit ripening. Plant J. **27:** 213–222.

Rodriguez-Concepcion, M., and Boronat, A. (2002). Elucidation of the methylerythritol phosphate pathway for isoprenoid biosynthesis in bacteria and plastids. A metabolic milestone achieved through genomics. Plant Physiol. **130:** 1079–1089.

Roemer, S., Fraser, P.D., Kiano, J.W., Shipton, C.A., Mills, P.B., Drake, R., Schuch, W., and Bramley, P.M. (2000). Elevation of the provitamin A content of transgenic tomato plants. Nat. Biotechnol. **18:** 666–669.

Ronen, G., Carmel-Goren, L., Zamir, D., and Hirschberg, J. (2000). An alternative pathway to beta-carotene formation in plant chromoplasts discovered by map-based cloning of Beta and old gold color mutations in tomato. Proc. Natl. Acad. Sci. USA **97:** 11102–11107.

Sambrook, J., Fritsch, E.F., and Maniatis, T. (1989). Molecular Cloning: A Laboratory Manual. (Cold Spring Harbor, NY: Cold Spring Harbor Laboratory Press).

Sauret-Gueto, S., Botella-Pavia, P., Flores-Perez, U., Martinez-Garcia, J.F., San Roman, C., Leon, P., Boronat, A., and Rodriguez-Concepcion, M. (2006). Plastid cues posttranscriptionally regulate the accumulation of key enzymes of the methylerythritol phosphate pathway in *Arabidopsis*. Plant Physiol. **141:** 75–84.

Schaub, P., Al-Babili, S., Drake, R., and Beyer, P. (2005). Why is golden rice golden (yellow) instead of red? Plant Physiol. **138:** 441–450.

Schwartz, S.H., Quin, X., and Zeevaart, J.A.D. (2003). Elucidation of the indirect pathway of abscisic acid biosynthesis by mutants, genes and enzymes. Plant Physiol. **131:** 1591–1601.

Shewmaker, C., Sheehy, J.A., Daley, M., Colburn, S., and Ke, D.Y. (1999). Seed-specific overexpression of phytoene synthase: Increase in carotenoids and other metabolic effects. Plant J. **20:** 401–412.

Simkin, A.J., Gaffé, J., Alcaraz, J.P., Carde, J.P., Bramley, P.M., Fraser, P.D., and Kuntz, M. (2007). Fibrillin influence on plastid ultrastructure and pigment content in tomato fruit. Phytochemistry **68:** 1545–1556.

Simkin, A.J., Schwartz, S.H., Auldridge, M., Taylor, M.G., and Klee, H.J. (2004). The tomato carotenoid cleavage dioxygenase 1 genes contribute to the formation of the flavour volatiles beta-ionone, pseudoionone and geranylacetone. Plant J. **40:** 882–892.

Télef, N., Stammitti-Bert, L., Mortain-Bertrand, A., Maucourt, M., Carde, P., Rolin, D., and Gallusci, P. (2006). Sucrose deficiency delays lycopene accumulation in tomato fruit pericarp discs. Plant Mol. Biol. **62:** 453–469.

Than, A., Bramley, P.M., Davies, B.H., and Rees, A.F. (1972). Stereochemistry of phytoene. Phytochemistry **11:** 3187–3192.

Tian, L., Musetti, V., Kim, J., Magallanes-Lundback, M., and DellaPenna, D. (2004). The *Arabidopsis* LUT1 locus encodes a member of the cytochrome P450 family that is required for carotenoid epsilon-ring hydroxylation activity. Proc. Natl. Acad. Sci. USA **101:** 402–407.

Valentin, H.E., Lincoln, K., Moshiri, F., Jensen, P.K., Qi, Q., Venkatesh, T.V., Karunanandaa, B., Baszis, S.R., Norris, S.R., Saidge, B., Gruys, K.J., and Last, R.L. (2006). The *Arabidopsis* vitamin E pathway gene 5-1 mutant reveals a critical role for phytol kinase in seed tocopherol biosynthesis. Plant Cell **18:** 212–224.